NRL REPORT 3855



# DESIGN OF THE AN/SPS-2 ANTENNA




NAVAL RESEARCH LABORATORY

WASHINGTON, D.C.

NRL REPORT 3855



# DESIGN OF THE AN/SPS-2 ANTENNA

R. J. Adams and J. R. Shoemaker

October 4, 1951

Approved by:

R. C. Guthrie, Head, Search Radar Branch
L. A. Gebhard, Superintendent, Radio Division II

NAVAL RESEARCH LABORATORY
CAPTAIN F. R. FURTH, USN, DIRECTOR
WASHINGTON, D.C.

[redacted]

## DISTRIBUTION

| | |
|---|---|
| OpNav | |
| Attn: Op-413B2 | 5 |
| Attn: Op-42 | 2 |
| Attn: Op-374 | 1 |
| ONR | |
| Attn: Code 470 | 1 |
| BuAer | |
| Attn: Code EL-43 | 2 |
| BuOrd | |
| Attn: Code RE4F | 2 |
| BuShips | |
| Attn: Code 820 | 10 |
| Attn: Code 833 | 1 |
| CO and Dir., USNEL | |
| Attn: Code 470 | 2 |
| Attn: Dr. T. J. Keary, Code 300 | 1 |
| CDR, USNOTS | |
| Attn: Reports Unit | 2 |
| Supt., USNPGS | 1 |
| CDR, NATC | |
| Attn: Electronics Test | 1 |
| Attn: Mr. R. L. Hensell | 1 |
| CDR, NADC | |
| Attn: Dr. H. Krutter | 2 |
| OinC, US Naval School, Naval Training Center, Great Lakes, Illinois | |
| Attn: Electronics Maintenance | 1 |
| OCSigO | |
| Attn: Ch. Eng. and Tech. Div., SIGTM-S | 1 |
| CG, SCEL | |
| Attn: SCEL Liaison Office | 3 |
| CG, Wright-Patterson AFB | |
| Attn: BAU-CADO | 1 |
| Attn: CADO-E1 | 2 |
| Attn: Ch., Electronics Subdiv., MCREEO-2 | 1 |





[redacted]

CONTENTS

## ABSTRACT

An antenna has been designed to meet the requirements of the final version of the AN/SPS-2 radar system. The paraboloidal reflector has a diamond contour 40 feet wide by 20 feet high and a focal length of 16 feet 3 inches. The feed assembly consists of an array of seven horns stacked in a vertical line through the focus.

During the transmitter pulse the horns are excited with the relative amplitudes and phases necessary to generate a vertical pattern giving constant-altitude coverage to an elevation angle of 21 degrees. Power division is accomplished with a 3-db directional coupler developed by H. J. Riblet. Phase adjustments are made with hairpin sections of waveguide.

When the magnetron is not firing, the seven horns are connected to separate receivers, and target height is computed from the video signals. Adjacent receiving beams cross at the 4-db levels, alternate beams at the 14-db level. The vertical (H-plane) aperture of the feed horns is chosen to maximize their directivity. The reflector is modified by the addition of a cylindrical phasing-strip to produce vertical patterns suitable for height finding. Transmitting, receiving, and composite contours of equal intensity are plotted.

The standing-wave ratio at the antenna input does not exceed 1.5 over the frequency band 1250 to 1350 Mc. The gain of the number 3 (on-axis) beam is 36.8 db, which represents an aperture efficiency of 52 percent.

A cavity-type monitor antenna is mounted at the vertex of the reflector.

## PROBLEM STATUS

This is a final report on one phase of the problem; work on other phases is continuing.

## AUTHORIZATION

NRL Problem R02-22R
RDB NE 050-503

Manuscript submitted for publication June 8, 1951.

# DESIGN OF THE AN/SPS-2 ANTENNA

## SYSTEM DESIGN

The AN/SPS-2 radar is a very-long-range search and height-finding set for use in detection and ship-controlled interception of aircraft and flat-trajectory missiles. The early development phases of this system have been reported previously.[1,2] As originally planned, the set was to have been capable of tracking such difficult targets as the German A-4 (V-2) missile by means of seven or eight 10-megawatt beams on separate frequencies, stacked in the vertical plane. An antenna was designed for this system,[3] and a model has been constructed and tested by the Raytheon Manufacturing Company.[4] In April 1948 the military characteristics of the AN/SPS-2 were revised to limit the required coverage to an altitude of 90,000 feet, and this made it possible to consider the use of a single 10-megawatt transmitter.

In the present design, the transmitted power is divided among seven beams as indicated in Table 1. By careful phasing of the feed horns, it is possible to generate a broad, vertical transmitting pattern which approximates the coverage desired. A separate receiver is provided for each of the beams, and elevation-angle information is derived from a comparison of video signals. Figure 1 shows the calculated detection contours for a nonscintillating target of 1-square-meter cross section. This chart is based on the SPS-2 parameters listed in Table 2, and on the observed performance of the SPS-6b, which gives a 50-percent blip-scan ratio on two VF's ($\sigma$ = 16m$^2$) at 60 nautical miles. Since the SPS-2 system enjoys an advantage of approximately 32 db, it should have a free-space range of 190 miles on a one-square-meter target lying in the direction of one of the three lowest beams. Figure 1 was obtained from this range by introducing the composite transmitting and receiving patterns. At any altitude up to 90,000 feet, the coverage extends to 170 miles and to an elevation angle of at least 21 degrees. The double lines associated with the first three beams are envelopes of the lobe structure arising from water reflection.

---

[1] Varela, A. A., "Proposed Very Long Range Radar with Height Finding," NRL Report 2759 (Restricted), February 18, 1946

[2] Varela, A. A., "Interim Report on the AN/SPS-2 (XDQ) Radar System," NRL Report R-3313 (Confidential), July 14, 1948

[3] Adams, R. J., Kelleher, K. S., and Lundquist, C. R., "Preliminary Design of the AN/SPS-2 (XDQ) Antenna," NRL Report R-3412 (Confidential), February 4, 1949

[4] Raytheon Manufacturing Company, "Final Development Report for Search Radar Equipment AN/SPS-2," Index No. NE 050515 (Confidential), June 30, 1950

TABLE 1
Power Division Ratios

| Beam Number | Elevation Angle | Relative Power Input |
|---|---|---|
| 1 | 1.1° | 0.25 |
| 2 | 4.1 | .25 |
| 3 | 7.1 | .25 |
| 4 | 10.1 | .125 |
| 5 | 13.1 | .062 |
| 6 | 16.3 | .031 |
| 7 | 20.0 | .031 |

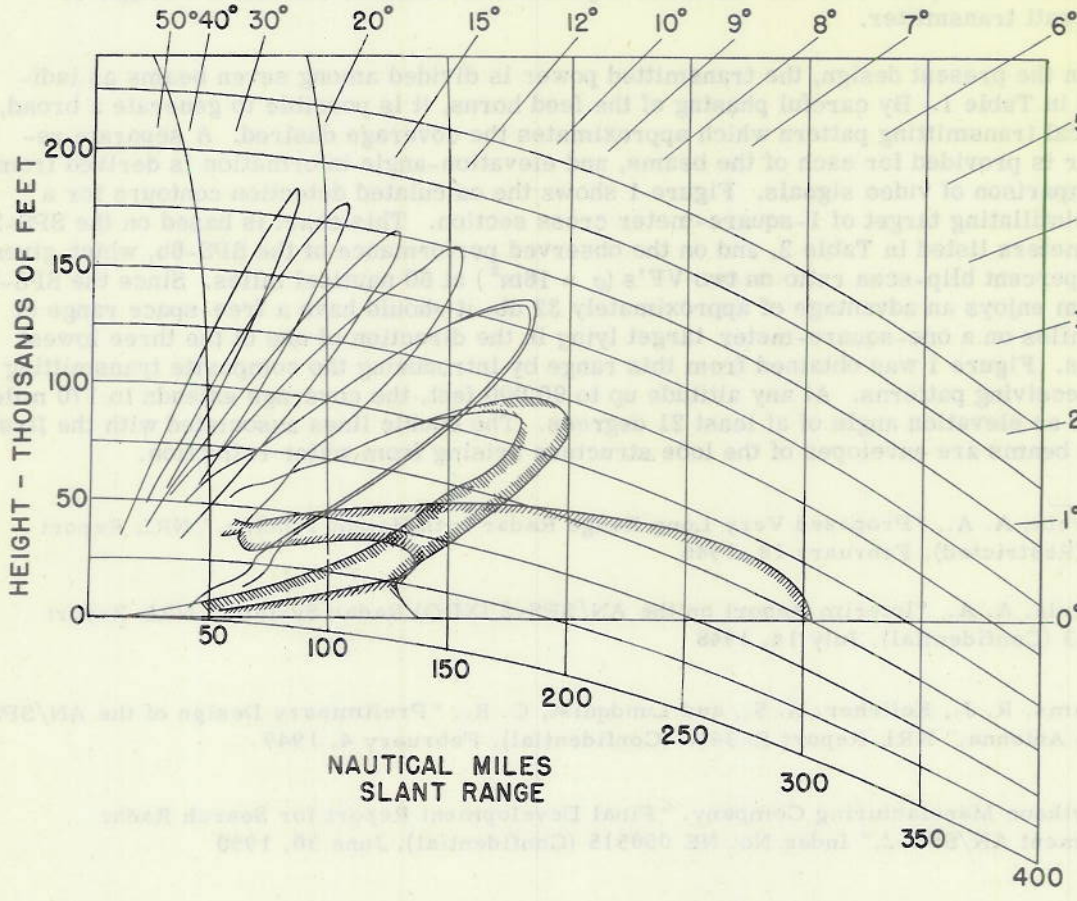


Figure 1 - Calculated range of detection versus height for AN/SPS-2 system

TABLE 2
AN/SPS-2 Parameters Affecting Detection Range

| | |
|---|---|
| Wavelength | 23 cm |
| Transmitted Power | 10 megw |
| Antenna Gain on Transmit ($2^\circ$ to $7^\circ$) | 32.1 db |
| Antenna Gain Receive (Beam 3) | 36.8 db |
| Pulse Length | 7 $\mu$s |
| Pulse Repetition Frequency | 244 pps |
| Receiver Noise Figure | 9.0 db |
| Duplexer and Transmission Line Loss | 2.5 db |
| Antenna Rotation Rate | 10 rpm |
| Horizontal Beamwidth | 1.6 deg |

## ANTENNA REQUIREMENTS

System considerations have led to the following design objectives for the AN/SPS-2 antenna:

1. The antenna width and height should be limited to 36 and 18 feet, and the focal length should be so chosen that the turning radius does not exceed 18 or 20 feet.

2. Seven horizontally polarized feeds should be provided whose individual secondary patterns in the horizontal and vertical planes have beam widths of approximately 1.6 and 2.5 degrees, respectively, and sidelobes below the 28 and 30 db levels. (The sidelobe level required for the vertical patterns has been set as low as seems possible of attainment in order to compensate for the fact that a broad transmitting pattern is used; a 30-db lobe in the receiving pattern is equivalent to a 15-db lobe in a conventional radar. In the horizontal plane the transmitting and receiving patterns are similar, so that a 28-db lobe gives 56-db discrimination. If the system sensitivity is just sufficient to detect a one-square-meter target at 240 miles, then a large bomber of 100 square meters cross section should give a signal at 30 miles (the maximum range of the STC) that is 56 db (20 + 4 x 9) above noise on the main beam and just visible on a 28-db sidelobe. Of course ship targets have cross sections far in excess of 100 square meters, but under standard atmospheric conditions they should not appear beyond 30 miles.)

3. Each of the four lower vertical patterns should cross its neighbor at the 4-db point or higher to ensure reasonably solid coverage.

(This corresponds to the 2-db requirement in the earlier multiple-frequency system.) In addition, the level at which each of these patterns crosses the center line of its neighbor should lie above 14 db. This is approximately the point at which alternate beams cross, and may be called a "second crossover" to distinguish it from the "first crossover" already considered. If the second crossover is too low, the height computer must compare widely differing signals, and the range to which the set will measure height is reduced. The two upper beams must be spaced more widely to extend the coverage to 21 degrees, and a slight deterioration in height-finding performance must be accepted.

4. The gain of each individual beam should be as close to

$$0.65\,\frac{4\pi A}{\lambda^2}$$

as the above conditions permit.

5. A waveguide circuit must be arranged to divide the transmitter power among the seven horns in the proportions indicated in Table 1, and with the proper phase relations to keep the transmitted pattern smooth and reasonably constant in shape throughout the 8-percent band from 1250 to 1350 Mc. The voltage standing wave ratio at the input to the power divider should not exceed 1.5.

## PRELIMINARY REFLECTOR DESIGN

The choice of a symmetrical reflector for the AN/SPS-2 antenna was governed by considerations described in an earlier report,[4] which may be summarized as follows. A reflector is preferred to a lens at L-band because it is lighter, easier to brace, and may have a smaller focal length for a given aperture. Further, a symmetrical reflector has better off-axis patterns and is better adapted to the use of multiple feeds than is one cut to an asymmetrical outline. The effects of feed obstruction on the pattern and of the reflector on mismatch are of relatively little importance for an antenna whose dimensions are large in comparison with the wavelength.

Development work on this antenna was carried out at X-band, with a model wavelength of 3.25 cm and a scaling factor to 1300 Mc of 7.10 (i.e., 23.08/3.25). The 8-percent band from 3.13 to 3.38 cm corresponds to the assigned band 1250 to 1350 Mc. The first reflector was a paraboloid of 27.5 inches focal length and had an elliptical outline—31 inches high by 60 inches wide—for which the corresponding L-band dimensions are 35′ 6″ wide by 18′ 4″ high by 16′ 3″ focal length. The width and height were chosen to satisfy the relations:

$$\theta_h = 1.60^\circ = 75^\circ \frac{\lambda}{W}\,, \qquad (1)$$

$$\theta_v = 2.50^\circ = 60^\circ \frac{\lambda}{H}\,, \qquad (2)$$

with the expectation that the illumination taper would be about 14 db in the horizontal plane and 5 db in the vertical plane. The choice of focal length is discussed in a later section.

 

Choice of H-Plane Aperture

In the present antenna a 4-db crossover is permissible, and larger horns may be used without going to an excessively great f/H ratio. Thus it has been possible to take advantage of the minimum at B, where the best horn aperture for an 8-percent band appears to be at $a = 1.175\lambda$, or 1.504 inches at $\lambda = 3.25$ cm.

Figure 3 is a photograph of the seven-horn feed system. The first five horns have H-plane apertures of 1.523 inches; those for the upper two beams have 2-inch apertures. The dimensions of the five similar horns are somewhat greater than planned because the partitions between them were filed to a knife edge after assembly.

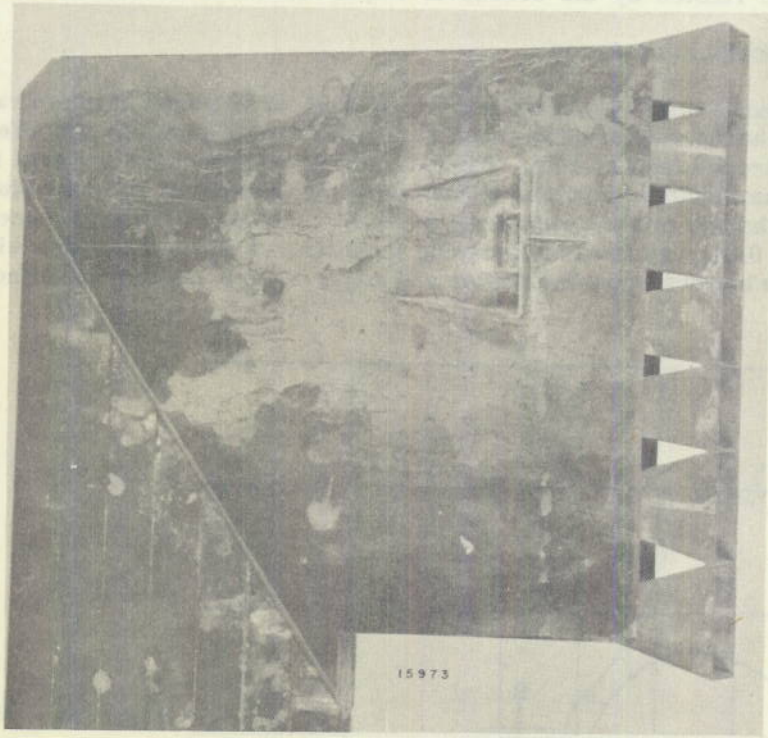


**Figure 3 - X-band model of feed-horn array for AN/SPS-2**

Figure 4 is a set of H-plane patterns for the number 3 horn taken at the center and edges of the frequency band. Their beamwidth at 5 db, indicated by the dashed line of Figure 2, is smallest at midband, but the agreement with the full curves is only approximate. This seems to indicate that the pattern of a horn in array is influenced by more distant horns as well as by its immediate neighbors. The patterns are noticeably flat near the axis, and as a consequence a greater fraction of the energy falls onto the reflector than would be the case for a pattern of normal shape.

Choice of Focal Length

The actual H-plane aperture of the horns is 1.523 inches, or 1.190 $\lambda$ at midband. Since a 4-db crossover is required, the f/H ratio should be 0.926. This is indicated by a cross

## FEED-HORN DESIGN

In a stacked-beam height-finding antenna the desired crossover level for adjacent beams fixes the feed separation in the vertical plane at such a small value that a waveguide horn of this size has insufficient directivity for proper illumination of the reflector. In fact, a 5-db taper between the center and top or bottom edges is about the largest that can be attained. For this reason it is appropriate to use the 5-db beamwidth of the vertical primary pattern as a measure of its directivity. A number of schemes have been investigated[5] which might be expected to increase the directivity of a horn of given aperture, but none of these has led to a practical design. It appears that the best available procedure is to adopt conventional waveguide horns, but to choose the f/H ratio and the horn aperture $a/\lambda$ —which are related by the crossover requirement—in the most advantageous way.

### Beamwidth of Horns in an Array

Figure 2 shows the H-plane beamwidth, at 5 db, of H-flared horns of various sizes. Arrays of three horns were used in these measurements to simulate the effect of neighboring horns in the extended feed system. The two curves represent the greatest and least values of beamwidth that could be obtained by adjusting the position of shorting plungers in the two outer horns. The two minima represent desirable choices of horn aperture. The one marked A, where $a/\lambda = 0.84$, was used in designing a multiple-frequency antenna with 2-db crossovers.[6] Three arrows mark the center and edges of an 8-percent frequency band.

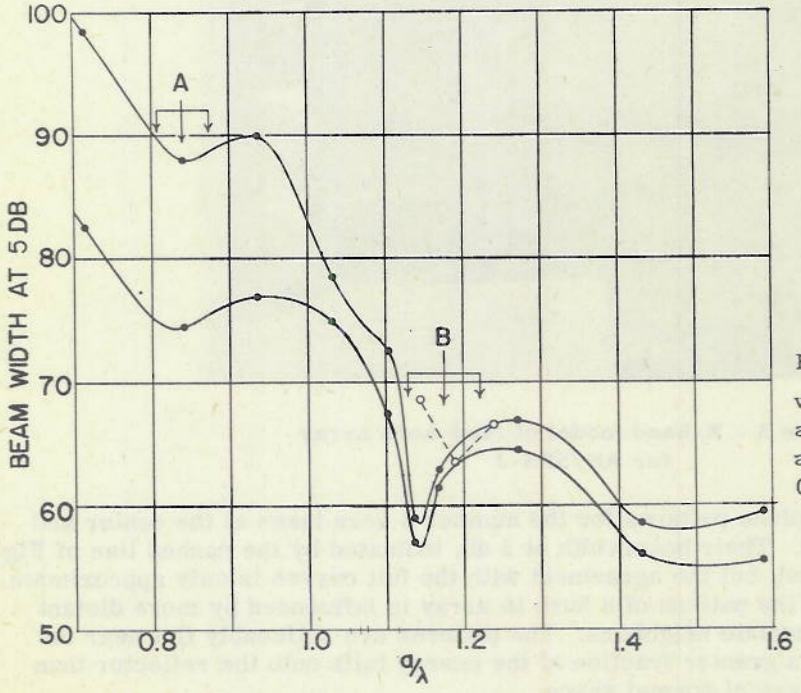


Figure 2 - H-plane beamwidth at 5 db vs. H-plane aperture for horns in an array (E-plane aperture 0.625 wavelengths)

[5] Adams, Kelleher, and Lundquist, op. cit., pp. 25-44

[6] Adams, Kelleher, and Lundquist, op. cit., p. 25

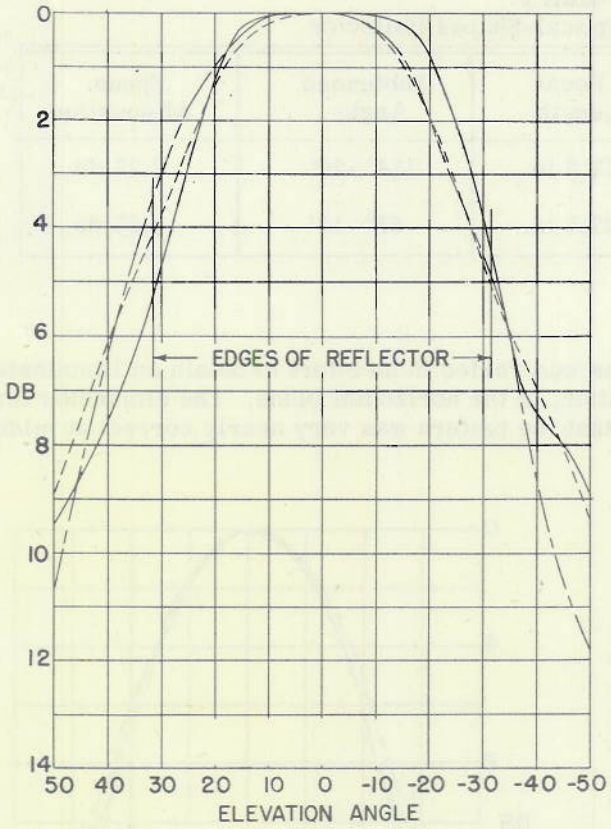


Figure 4 - H-plane primary patterns of No. 3 horn at three wavelengths
- - - - $\lambda$ = 3.13 cm
——— $\lambda$ = 3.25 cm
— - — $\lambda$ = 3.38 cm

on Figure 5, which was prepared from empirical data in a manner similar to that used for Figure 16 of NRL Report R-3412. If the reflector height is 31 inches, the focal length should be 28.71 inches. The nearest focal length available in spun aluminum dishes is 27.5 inches, and this was adopted for convenience. The horn aperture should have been reduced to compensate, as indicated by the lower cross in Figure 5, but it seems more important to take full advantage of the region of optimum directivity. Fortunately, with the existing feed system, the crossovers came out slightly higher than 4 db.

When the focal length had been chosen, the angles subtended by the reflector at its focus and the space attenuation in the principal planes could be computed. These are listed in Table 3.

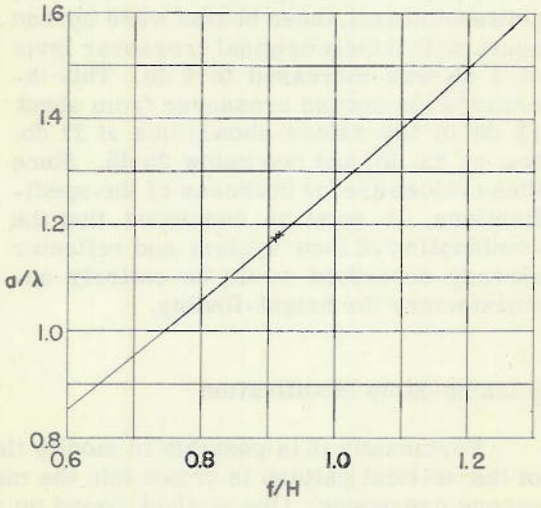


Figure 5 - Horn aperture as a function of f/H ratio for a 4-db crossover

[redacted]

TABLE 3
Dimensions of Elliptical-Shaped Reflector

| Plane | Aperture | Focal Length | Subtended Angle | Space Attenuation |
|---|---|---|---|---|
| Horizontal | 60 in. | 27.5 in. | $114^0$ -26′ | 2.27 db |
| Vertical | 31 in. | 27.5 in. | $63^0$ -10′ | 0.67 db |

Choice of E-Plane Aperture

The E-plane aperture of the feed horns was varied in an effort to obtain an illumination taper of 14 db, including the space attenuation, in the horizontal plane. The dimension finally chosen was 1.164 inches; Figure 6 shows that the pattern was very nearly correct at midband.

## REFLECTOR MODIFICATIONS

### Vertical Patterns of Original Reflector

A set of vertical patterns which show a crossover between adjacent beams at the 4-db level does not necessarily have a crossover between alternate beams at the 12- to 14-db level required for good height-finding performance. This is illustrated in Figure 7, where the vertical patterns of a 60-3/4- by 24-inch paraboloid of elliptic contour with a 21.1-inch focus have been replotted from Figure 62 of NRL Report 3412. On the assumption that the pattern shape varies slowly with crossover level, these beams were spread apart so that their original crossover level of 3 db was increased to 4 db. This increased the second crossover from about 13 db to the values shown: one at 21 db, two at 23 db, and two below 25 db. Since these values are far in excess of the specifications, it must be concluded that the combination of feed system and reflector already described would be entirely unsatisfactory for height-finding.

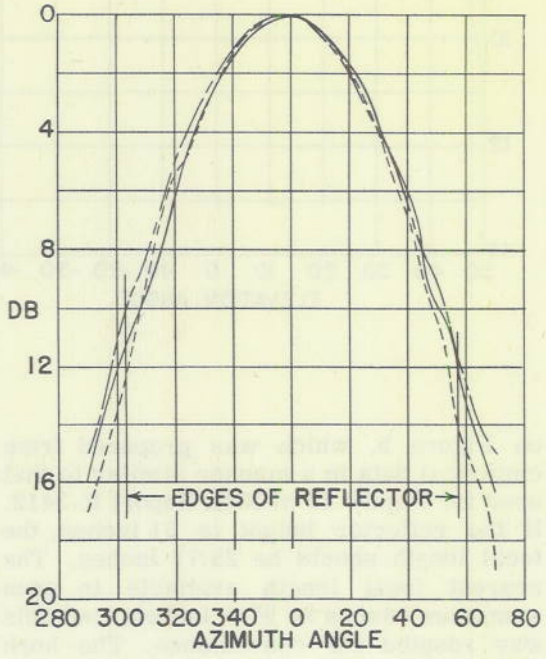


Figure 6 - E-plane primary patterns of No. 3 horn at three wavelengths: ----3.13 cm, ——3.25 cm, – – –3.38 cm

### Phasing-Strip Modification

Fortunately it is possible to modify the reflector in such a way that the first sidelobe of the vertical pattern is drawn into the main beam as a shoulder, raising the level of the second crossover. One method, based on a suggestion by L. C. Van Atta, consists of splitting the reflector horizontally through the vertex, and separating the two halves with a parabolic cylinder about a wavelength high. Since the axes of the two parts of the reflector

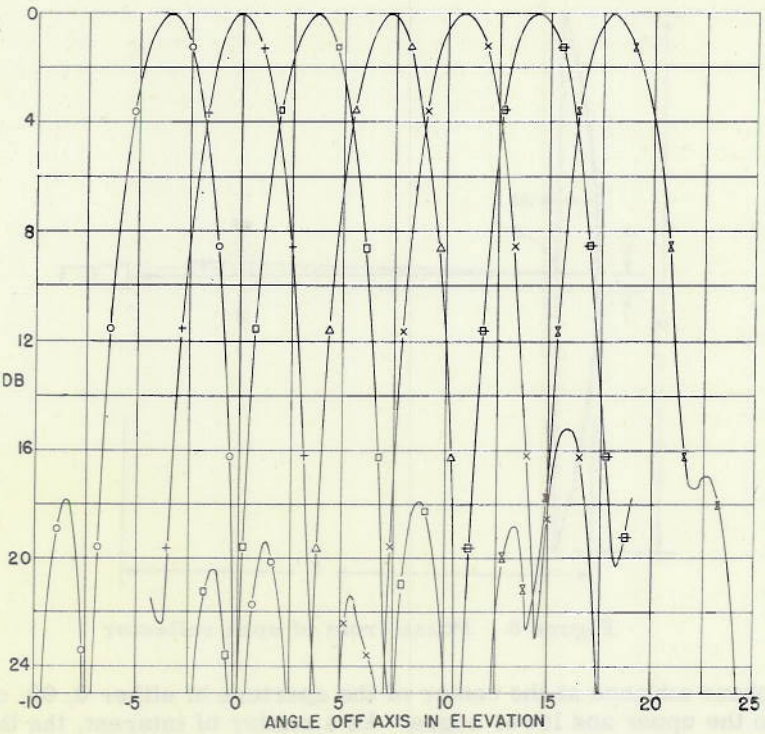


Figure 7 - Vertical patterns of elliptical reflector, replotted to 4-db crossovers

are offset, two beams, which travel in slightly different directions, are generated. Stated otherwise, there is a gabled phase distribution across the aperture as suggested by Figure 8. If the heights of the reflector and cylindrical strip are H and d respectively, then the phase deviation between the center and extremities of the reflector is:

$$\beta = \frac{360^\circ}{\lambda}\delta = \frac{360^\circ}{\lambda} \cdot \frac{H}{2} \cdot B\theta = \frac{360^\circ}{\lambda} \cdot \frac{H}{2} \cdot B \cdot \frac{d/2}{f},$$

$$\beta = 90^\circ \cdot \frac{d}{\lambda} \cdot \frac{B}{f/H} \cdot \qquad (3)$$

Since f/H = 0.887 and the beam factor B = 0.92 for this antenna, it is found that

$$\beta = 93.3^\circ \frac{d}{\lambda} \approx 90^\circ \frac{d}{\lambda}. \qquad (4)$$

Theory of Phasing-Strip in Rectangular Aperture

The best value for the phasing-strip height, d, has been determined in an approximate manner by means of pattern calculations. For this purpose the reflector shape was taken as rectangular, even though the actual contour was elliptical (and later diamond-shaped). A vertical illumination taper of 14 db rather than the actual value of 5 db was assumed in order to compensate to some extent for the effective taper due to the contour. The phase of the illumination was taken to be uniform in the horizontal, but gabled in the vertical

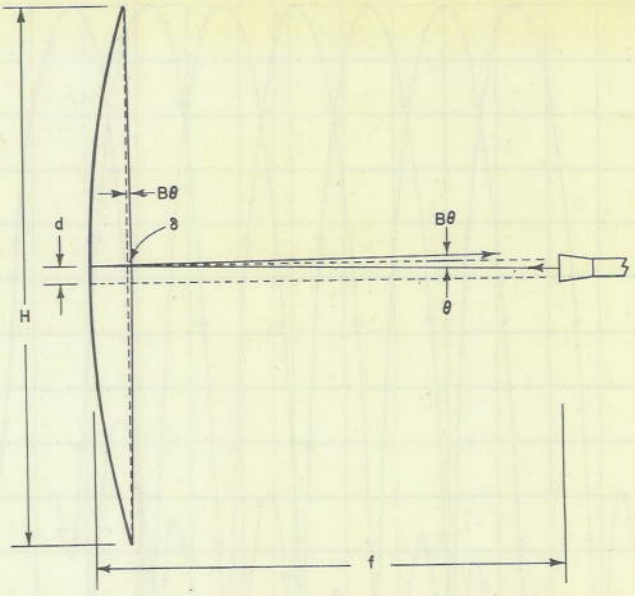


Figure 8 - Phase front of split reflector

plane, with a phase advance at the center of the aperture of either 0, 90, or 180 degrees with respect to the upper and lower edges. As a matter of interest, the three corresponding patterns for uniform illumination were also computed, and all six are shown in Figures 9, 10, and 11. Table 4 summarizes the results.

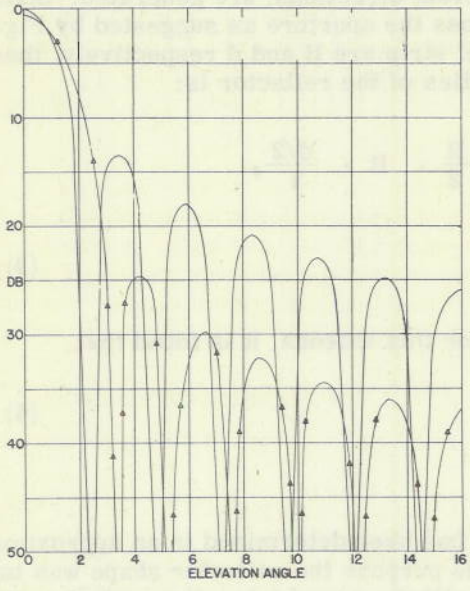


Figure 9 - Theoretical patterns of rectangular aperture with uniform phase: ——— uniform amplitude, —△— 14-db $\cos^2$ amplitude taper

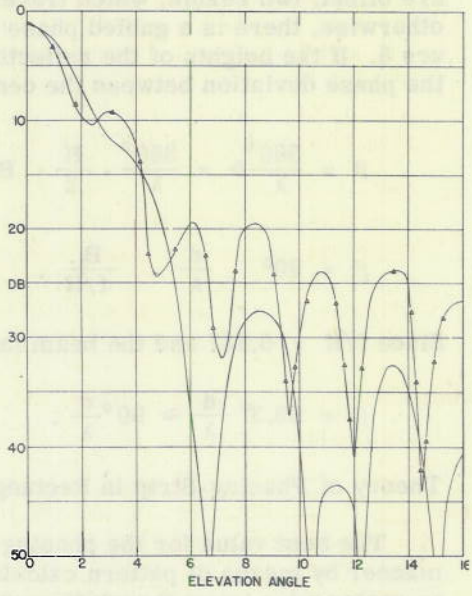


Figure 10 - Theoretical patterns of rectangular aperture with 90° phase-gabling: ——— uniform amplitude, —△— 14-db $\cos^2$ amplitude taper

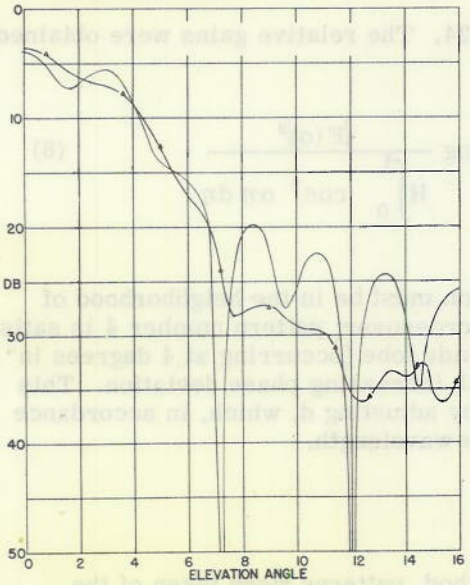


Figure 11 - Theoretical patterns of rectangular aperture with 180° phase-gabling:
——— uniform amplitude
—△— 14-db $\cos^2$ amplitude taper

TABLE 4
Pattern and Gain Characteristics of a Gabled-Phase Rectangular Aperture

| Pattern Number | Illumination Taper | Phase Deviation | H/λ x 3 db Beamwidth | Level* of 2nd Crossover | Relative Gain |
|---|---|---|---|---|---|
| 1 | 0 db | 90° | 52° | 50 db | 0.00 db |
| 2 | 14 | 0 | 64 | 30 | -0.57 |
| 3 | 0 | 90 | 52 | 10.4 | -0.91 |
| 4 | 14 | 90 | 70 | 12.2 | -1.29 |
| 5 | 0 | 180 | 174 | 25 | -3.92 |
| 6 | 14 | 180 | 152 | 21.4 | -3.62 |

* Assuming the first crossover is at the 4 db level.

The patterns were calculated from the integral

$$F(\theta) = R(\theta) + jI(\theta) = \int_{-\frac{1}{2}H}^{\frac{1}{2}H} \cos^2\left(\alpha\frac{2y}{H}\right) e^{j\left(\frac{2\pi}{\lambda} y \sin\theta - \beta\frac{2|y|}{H}\right)} dy \qquad (5)$$

where $\alpha$ takes on values of 0 and 63°-26′ and $\beta = 0, \frac{\pi}{2}$, or $\pi$. The resulting formulas are

$$R = \sum_{i=1,2} \frac{\frac{1}{2}H}{4\alpha^2 - \psi_i^2}\left[2\frac{\sin\psi_i}{\psi_i}\alpha^2 - \psi_i \sin\psi_i \cos^2\alpha + \cos\psi_i \cdot \alpha \sin 2\alpha\right] \qquad (6)$$

$$I = \sum_{i=1,2} \frac{\frac{1}{2}H}{4\alpha^2 - \psi_i^2}\left[2\frac{\cos\psi_i - 1}{\psi_i}\alpha^2 - \psi_i \cos\psi_i \cos^2\alpha - \sin\psi_i \cdot \alpha \sin 2\alpha + \psi_i\right] \qquad (7)$$

where $\psi_{1,2} = \beta \pm H\pi/\lambda \sin\theta$. $H/\lambda$ was taken equal to 24. The relative gains were obtained from the relation

$$G_{db} = 10 \log \frac{|F(o)|^2}{\int_{-\frac{1}{2}H}^{\frac{1}{2}H} \cos^4\left(\alpha \frac{2y}{H}\right) dy} = 10 \log \frac{|F(o)|^2}{H\int_0^1 \cos^4 \alpha\eta \, d\eta} . \quad (8)$$

Inspection of Table 4 shows that the phase deviation must be in the heighborhood of 90 degrees to produce the desired level at the second crossover; pattern number 4 is satisfactory in all respects. It will be noted that the first side lobe (occurring at 4 degrees in Figure 9) changes to a shoulder, whose level rises with increasing phase deviation. This means that the second-crossover level can be varied by adjusting d, which, in accordance with Equation (4), should be approximately equal to the wavelength.

## Tests of Elliptical Reflector with Phasing-Strip

As an experimental test of the split-reflector method, patterns were taken of the 60 x 31 inch (27.5-inch focus) reflector, with the feed system shown in Figure 3 and a succession of phasing strips varying in height from 1/2 to 2 inches. The patterns shown in Figure 12 for a 1-inch strip are fairly representative.

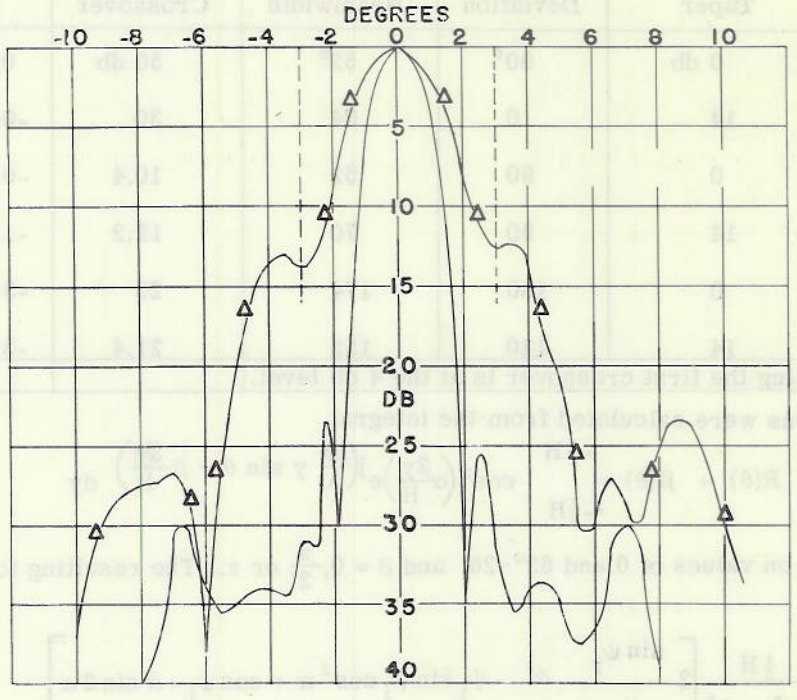


Figure 12 - Patterns of elliptical reflector with phasing strip inserted:
——— horizontal pattern
—△— vertical pattern

The vertical pattern has an acceptable second-crossover level of 13 db, as indicated by the vertical dashed lines, which are offset from the axis by one 4-db beamwidth. However, the shoulders predicted by the rectangular-aperture theory have the appearance of lobes, and the other sidelobes are objectionably high. A comparison with the two curves of Figure 10. suggests that a greater illumination taper in the vertical plane would be desirable.

The sidelobes in the horizontal pattern are likewise too high, in spite of the fact that pattern calculations for an elliptical aperture[7] indicate a maximum sidelobe of 32 db under approximately these conditions of illumination. There was no significant change in the pattern with the height of the strip. The reason for this discrepancy was not determined, but it seemed likely that it would be advantageous to increase the taper in the horizontal plane as well.

Since there seemed to be little prospect of improving the illumination taper by changing the feed-horn dimensions, an attempt was made to accomplish the same result by altering the reflector contour.

## Choice of Diamond Contour

Previous experience had indicated that covering a portion of a paraboloidal reflector with absorbent material designed for the operating wavelength was electrically equivalent to removing that part of the reflector. Thus it was an easy matter to experiment with contours contained within the original ellipse. Three such contours are shown in Figure 13, and correspondnig H- and E-plane patterns in Figures 14 and 15. When reflecting area was removed from the "corners" as in Figure 13C, the vertical patterns improved steadily, especially in the development of smooth shoulders near the second crossover point, but the horizontal patterns passed through an optimum at contour B. The dashed curves of Figures 14 and 15 show that the latter configuration suppressed the sidelobes to 30 db in both planes, and this led to final adoption of the diamond reflector. Ultimately small triangles were removed from the top and bottom by means of horizontal cuts 2-1/2 inches long.

At this point of the development it was realized that seven pairs of UG-39/U and UG-40/U waveguide connectors, originally inserted between the feed horns and the first mitered corner, had a most serious effect on the horizontal patterns. The full and dashed curves of Figure 16, obtained with and without this vertical line of connectors, demonstrate that they were responsible for a number

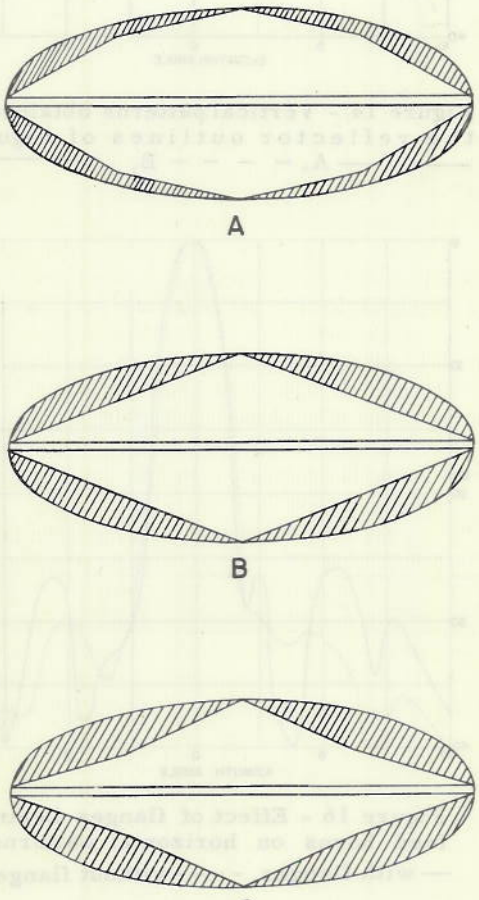


Figure 13 - Experimental reflector outlines

[7] Adams, R. J., and Kelleher, K. S., "Pattern Calculations for Antennas of Elliptical Aperture (Abstract)," Proc. I.R.E., 38; 1052, September 1950

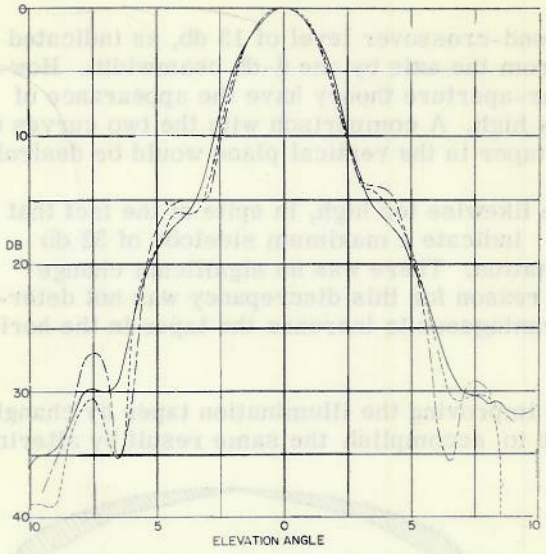


Figure 14 - Vertical patterns obtained with the reflector outlines of Figure 13: —— – —— A, – – – – B, ———— C

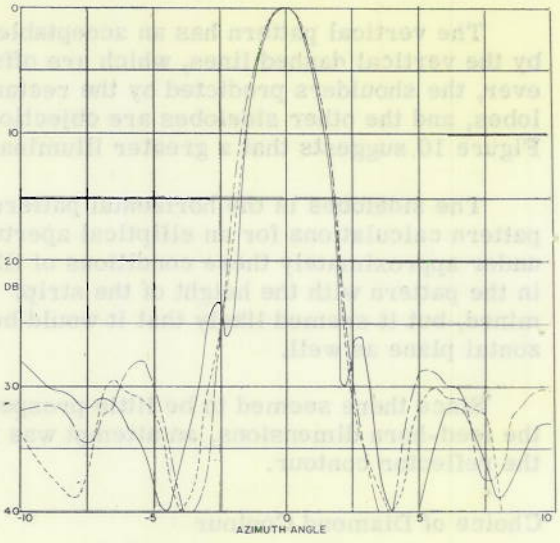


Figure 15 - Horizontal patterns obtained with the reflector outlines of Figure 13: ———— A, – – – – B, —— —— C

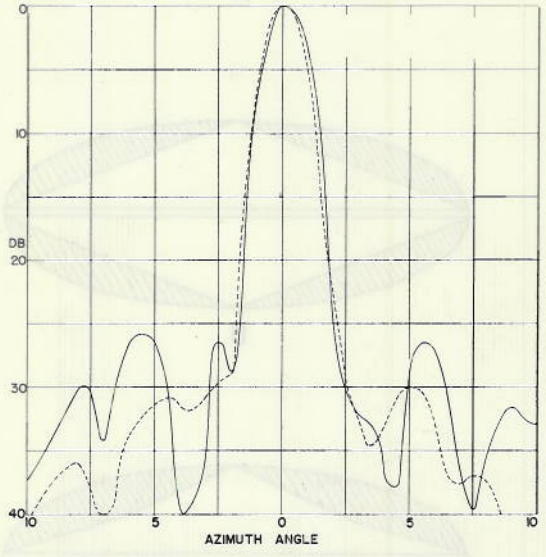


Figure 16 - Effect of flanges behind feed horns on horizontal patterns: — with flanges, - - - - without flanges

of lobes at the 26- or 27-db level. This may explain the high sidelobes observed with the elliptical contour, but experimental records are incomplete on this point. In any case, it is evident that great care must be exercised to keep the silhouette of the feed-horn array to a minimum.

## Readjustment of Reflector Dimensions

Since contour B reduces the reflector area from that of the ellipse in the ratio of 2 to $\pi$, the gain may be expected to drop in proportion (i.e., by 2 db), while the beams broaden by 25 percent in both planes. This effect was offset to some extent by increasing the reflector width and height from 60 x 31 inches to 67.6 x 33.8 inches, thus bringing the gain within 0.8 db of the elliptical dish, and the beamwidths to a value only 10 percent greater. The focal length was maintained at 27.5 inches. Figures 17 and 18 show the final appearance of the X-band model of the antenna.

Although this modification increases the full-scale aperture dimensions to 40 feet by 20 feet, the mechanical problem is not aggravated, for the wind forces are reduced in proportion to the area, and there may be a saving of weight in the fact that the structure is distributed approximately as in a cantilever beam of uniform strength.

Figure 17 - Front view of X-band model of antenna

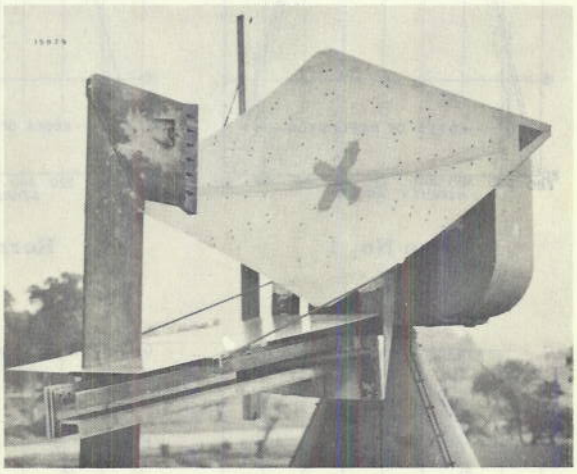

Figure 18 - Three-quarter view of antenna, modified to simulate mechanical features of L-band design (see Figure 73)

## RECEIVING CHARACTERISTICS OF THE ANTENNA

In describing the r-f performance of the X-band model of the AN/SPS-2 antenna, it is convenient to consider first the properties of the individual beams utilized by the radar in the receiving condition, and then the characteristics of the transmitting pattern obtained by combining these beams.

### Primary Patterns

The feed-horn assembly already described was used without change in the diamond-shaped reflector, since both the crossover level in the vertical patterns and the horizontal illumination taper were satisfactory. E- and H-plane primary patterns of all seven horns are shown in Figures 19 and 20 respectively, together with vertical lines marking the angular limits of the reflector. The horns are numbered consecutively from the top so as to correspond to the numbering of beams from the water upward. Horn No. 3, which is centered on the axis of the reflector, gives an illumination taper, at mid-band, of 6.7 db to the top and bottom edges, including a space attenuation of 0.8 db, and 16.2 db to the sides, where the space attenuation is 2.8 db. Since the feeds are stacked vertically, the illumination at the top and bottom of the reflector varies from horn to horn, but the illumination at the sides is practically the same for all seven.

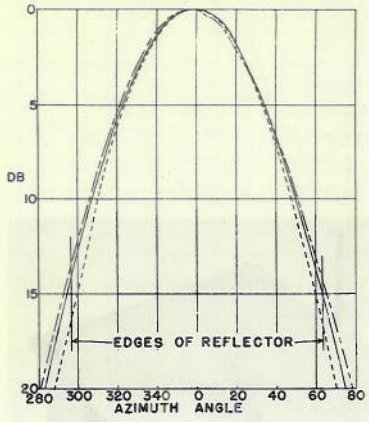


Horn No. 1

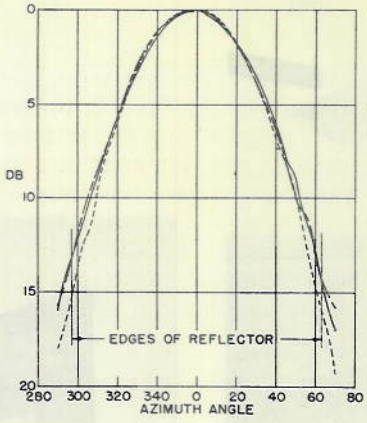


Horn No. 2

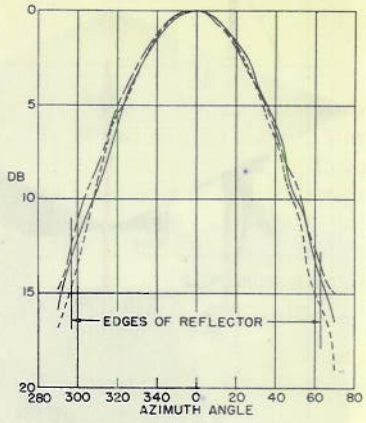


Horn No. 3

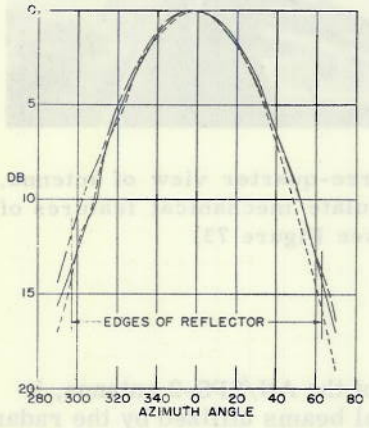


Horn No. 4

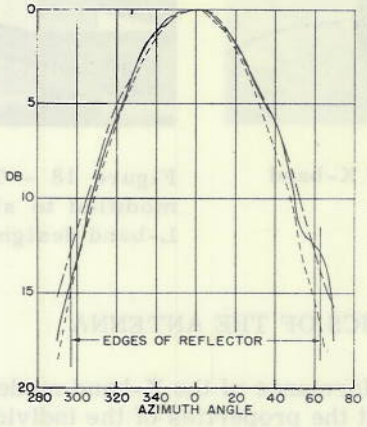


Horn No. 5

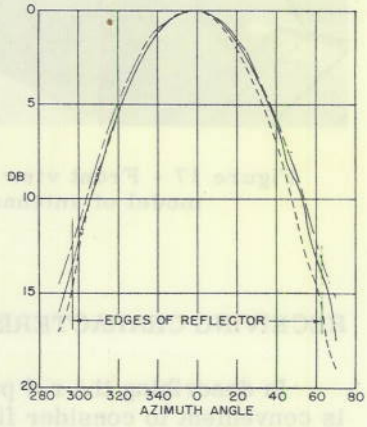


Horn No. 6

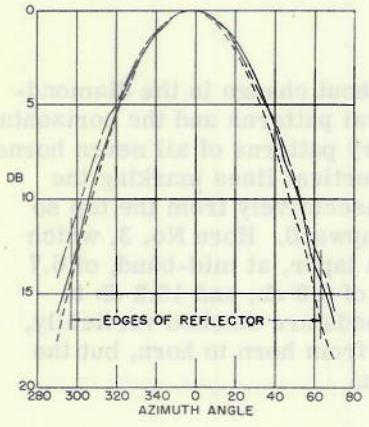


Horn No. 7

Figure 19 - Horizontal primary patterns of the seven feed horns. Wavelengths: ------3.13 cm, ———3.25 cm, — - —3.38 cm.

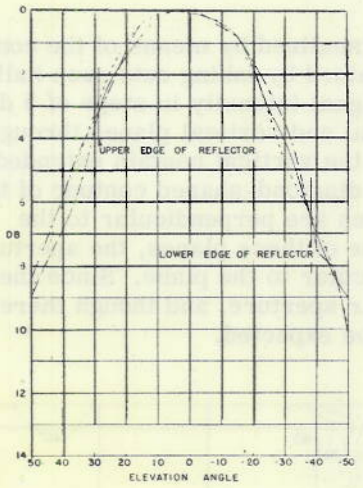


Horn No. 1

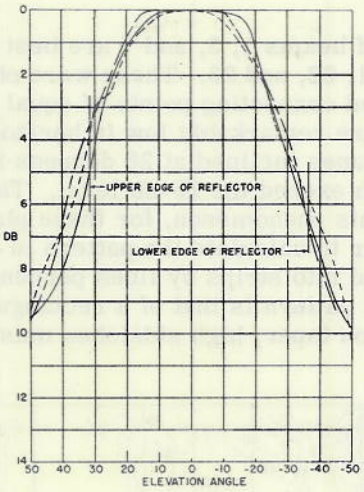


Horn No. 2

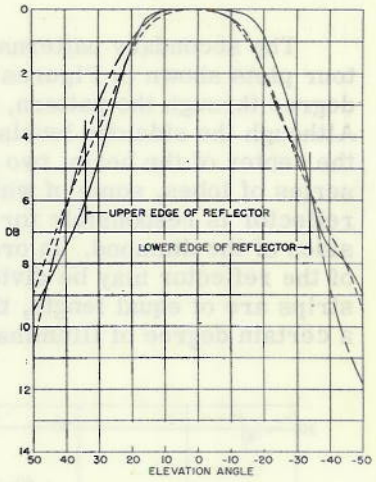


Horn No. 3

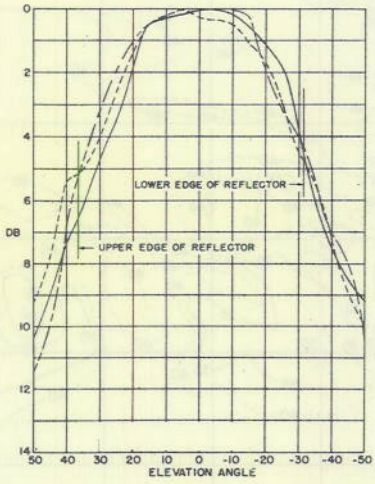


Horn No. 4

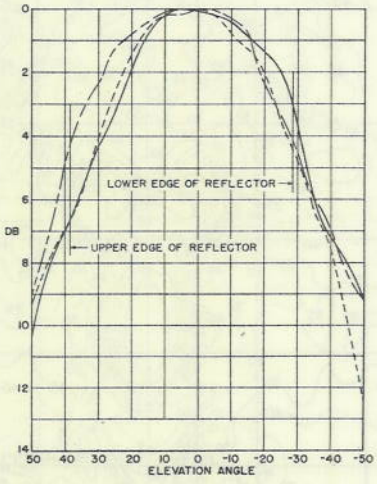


Horn No. 5

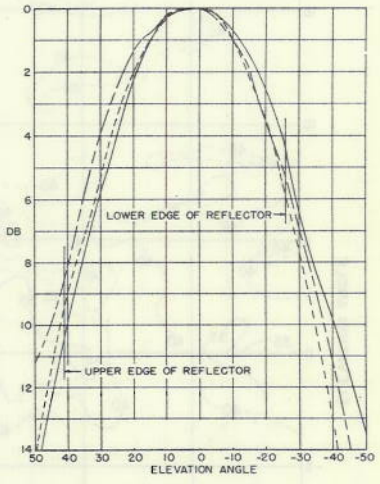


Horn No. 6

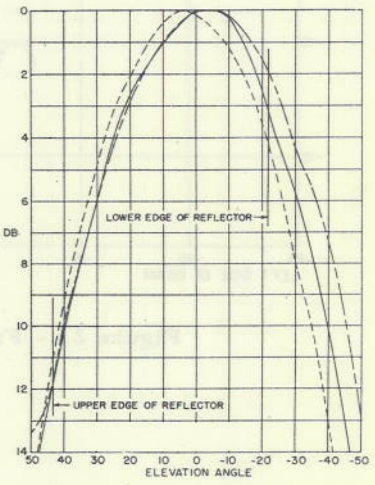


Horn No. 7

Figure 20 - Vertical primary patterns of the seven feed horns. Wavelengths: ----3.13 cm, —— 3.25 cm, —- - 3.38 cm.

Far-Field Contours

The secondary patterns of beams 1, 3, and 7 are best visualized by means of the contour plots shown in Figures 21, 22, and 23. These were obtained by taking cuts each half-degree through the pattern, and connecting points of equal signal intensity in steps of 5 db. Although the sidelobe levels are remarkably low in horizontal and vertical planes through the center of the beam, two planes inclined at 26 degrees to the vertical contain extended series of lobes, some of which exceed the 25-db level. The diamond-shaped contour of the reflector is responsible for this phenomenon, for these planes are perpendicular to the sides of the diamond. In order to calculate the pattern in one of these planes, the aperture of the reflector may be divided into strips by lines perpendicular to the plane. Since these strips are of equal length, the pattern is that of a rectangular aperture, and though there is a certain degree of illumination taper, high sidelobes must be expected.

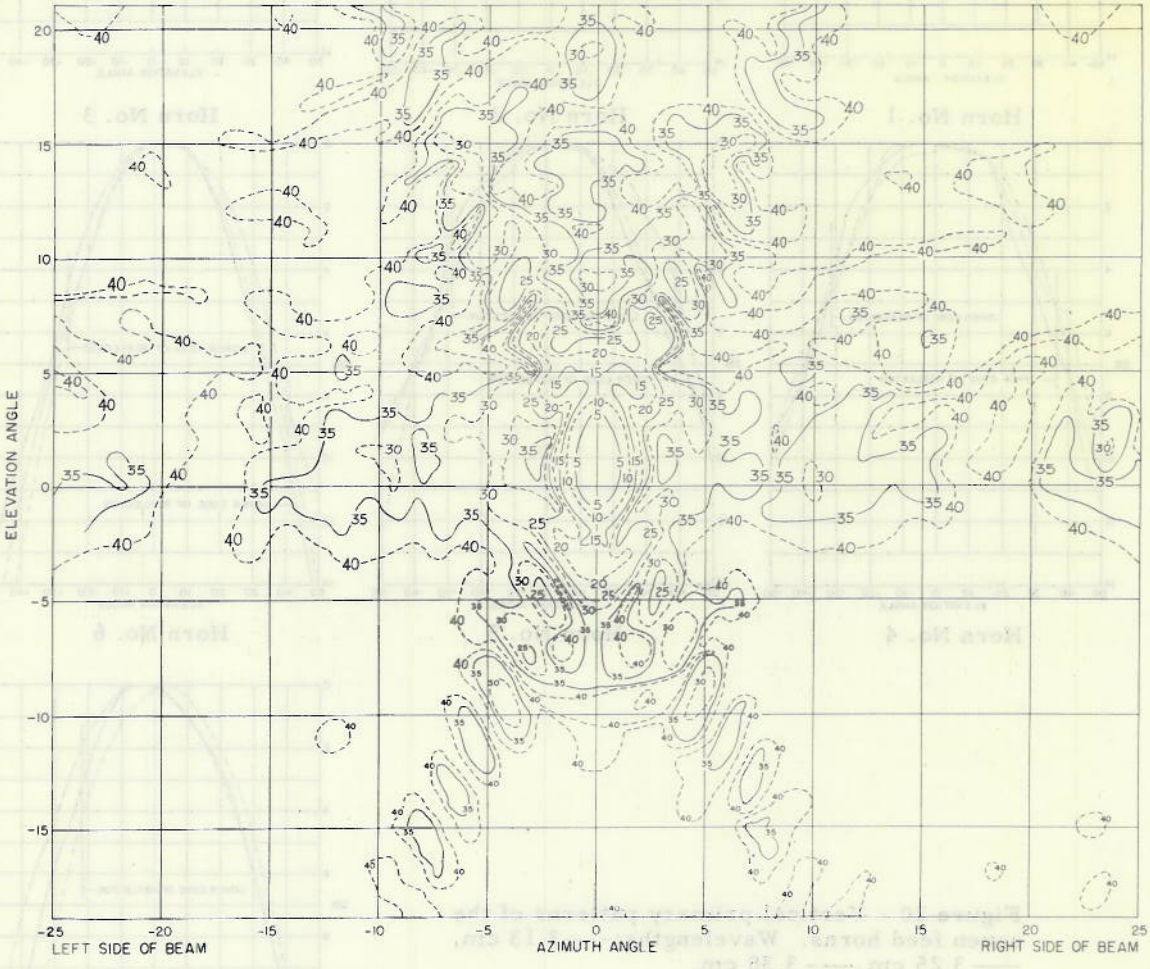


Figure 21 - Free-space equal-intensity contours of No. 1 beam

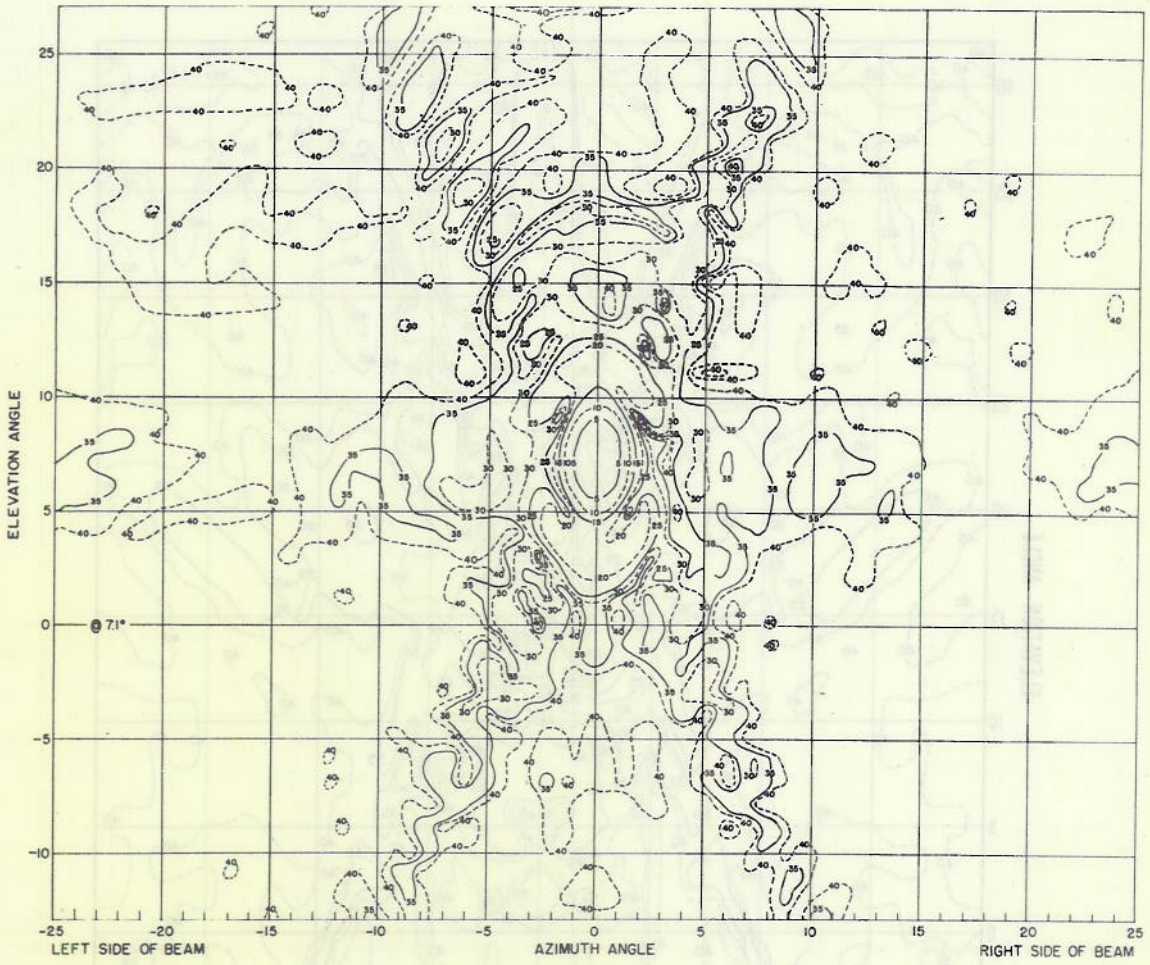


Figure 22 - Free-space equal-intensity contours of No. 3 beam

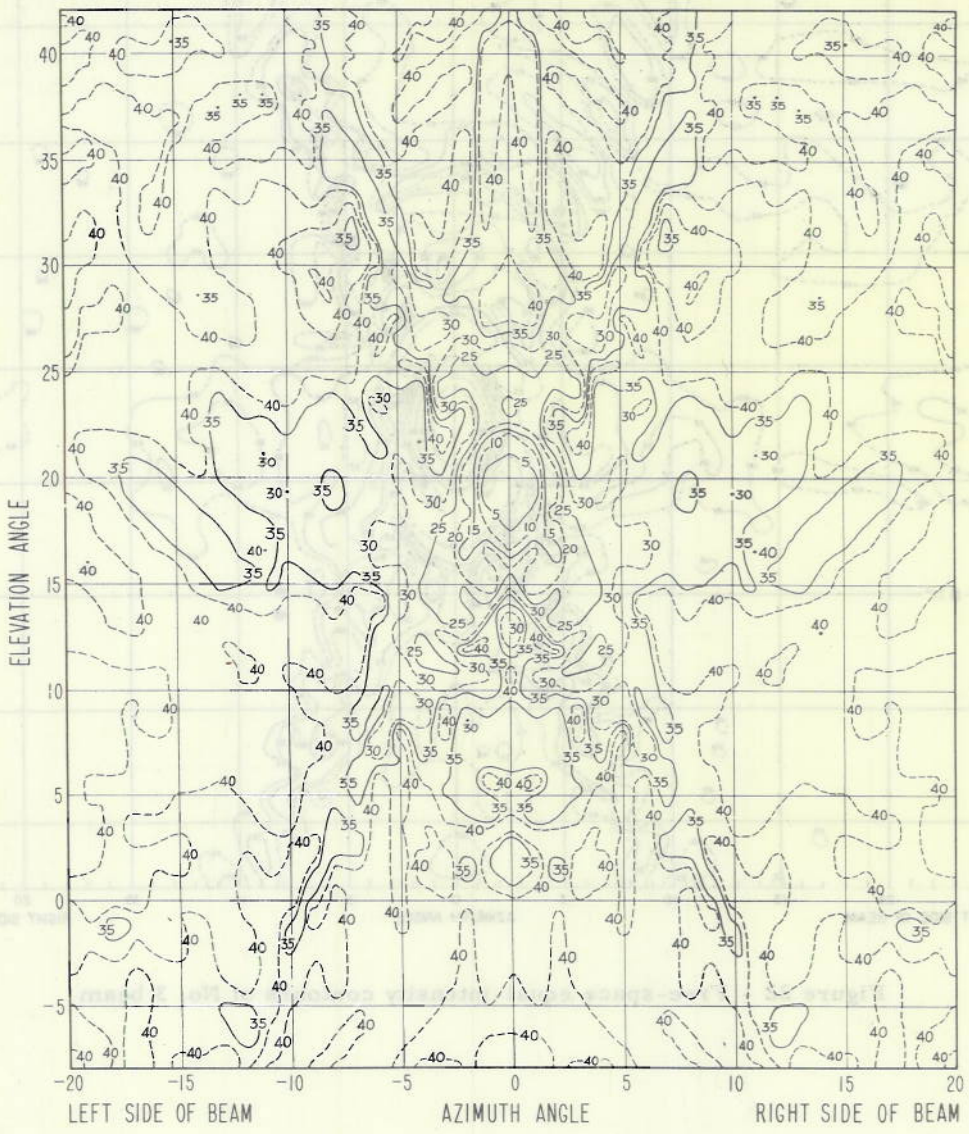


Figure 23 - Free-space equal-intensity contours of No. 7 beam

The contours of beams 1 and 3 have been replotted in Figures 24 and 25, with the effect of reflections from the surface of the sea taken into account. The contours refer to the envelope of the interference maxima. Beam No. 7 is unaffected by the water. While there is a tendency for the interference phenomenon to suppress sidelobes lying in inclined planes (unless two such lobes are disposed at equal angles above and below the horizon), the resulting patterns would be poorly adapted to a high-powered radar if used for both transmission and reception. Fortunately, as will be seen in a later paragraph, the objectionable lobes of the transmitting pattern do not coincide with those of the lower individual beams.

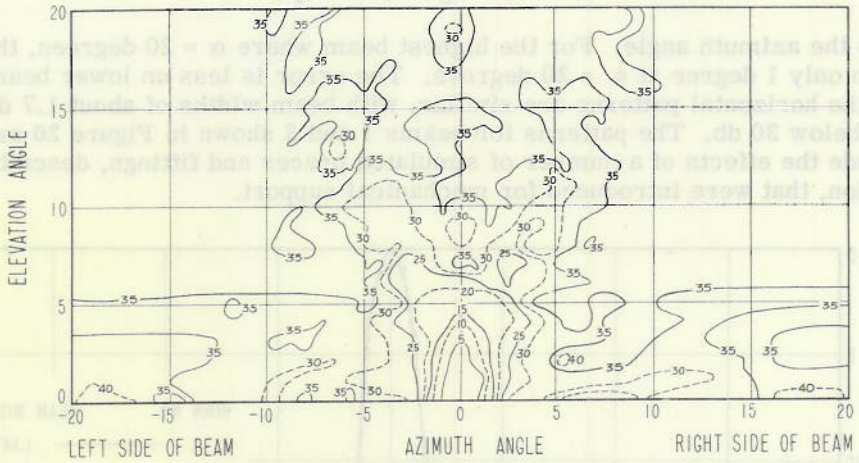


Figure 24 - Equal-intensity contours of No. 1 beam after correction for reflection from the water

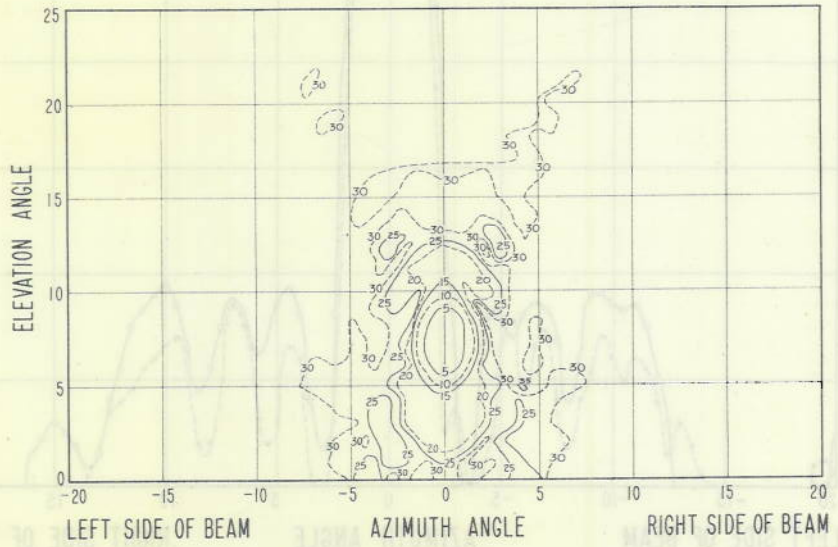


Figure 25 - Equal-intensity contours of No. 3 beam after correction for reflection from the water

Horizontal Patterns

Ideally, the horizontal patterns of the various beams should be measured along circles of latitude corresponding to their actual elevation angles, since this would indicate the signal variations to be expected as the beam sweeps through an elevated target. Unfortunately such a measurement procedure would require raising the transmitting antenna at the far end of the pattern range to considerable heights. It is much easier to re-level the antenna model and take great-circle patterns through each of the beams. The deviation from constant elevation is

$$\Delta\alpha = \alpha - \tan^{-1} [\cos \phi \tan \alpha] , \qquad (9)$$

where $\phi$ is the azimuth angle. For the highest beam where $\alpha$ = 20 degrees, the deviation amounts to only 1 degree at $\phi$ = 20 degrees. The error is less on lower beams. Taken in this way, the horizontal patterns are similar, with beam widths of about 1.7 degrees and sidelobes below 30 db. The patterns for beams 1 and 3 shown in Figure 26 are typical. They include the effects of a number of simulated braces and fittings, described in a later section, that were introduced for mechanical support.

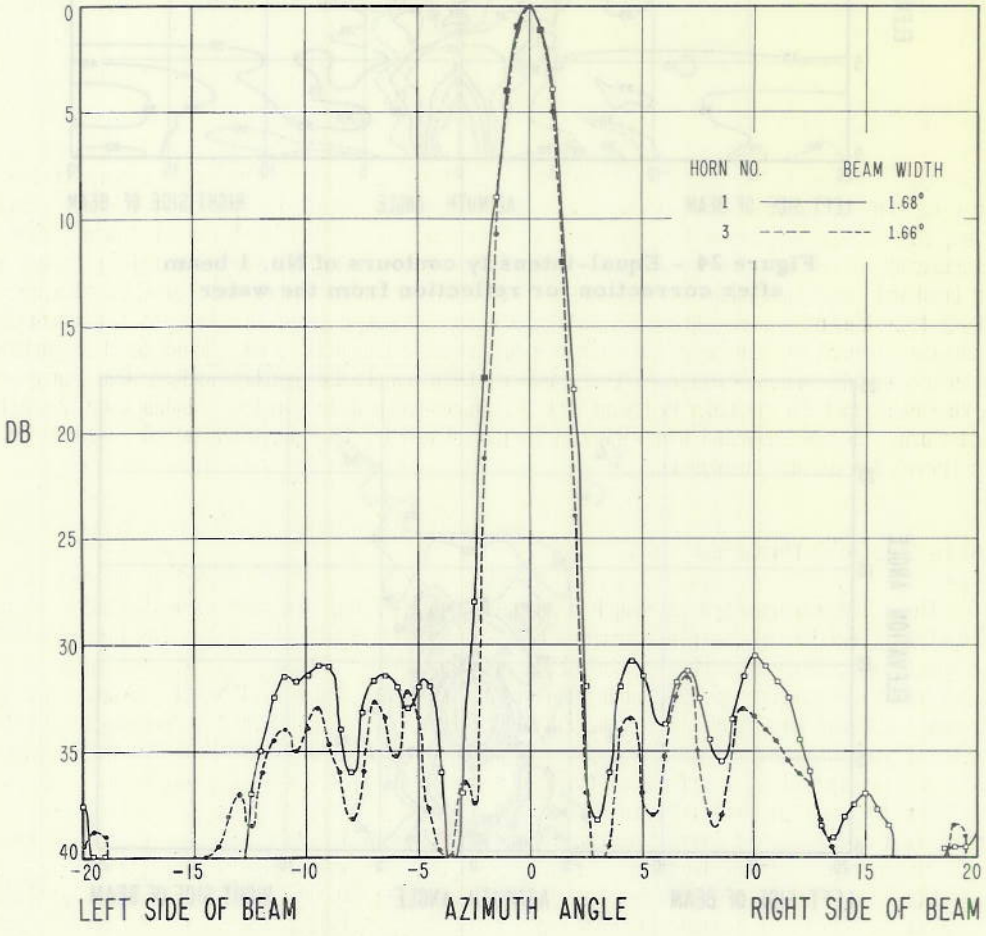


Figure 26 - Final horizontal patterns for beams 1 and 3

## Vertical Patterns

The vertical patterns in Figures 27 through 38 were taken at the center and edges of the frequency band with phasing-strip heights of 3/4, 1, 1-1/4, and 1-1/2 inches for the purpose of establishing the optimum value of this parameter. It appears that heights of 1 and 1-1/4 inches are equally satisfactory as regards the first and second crossover levels, pattern shape, and general sidelobe level.

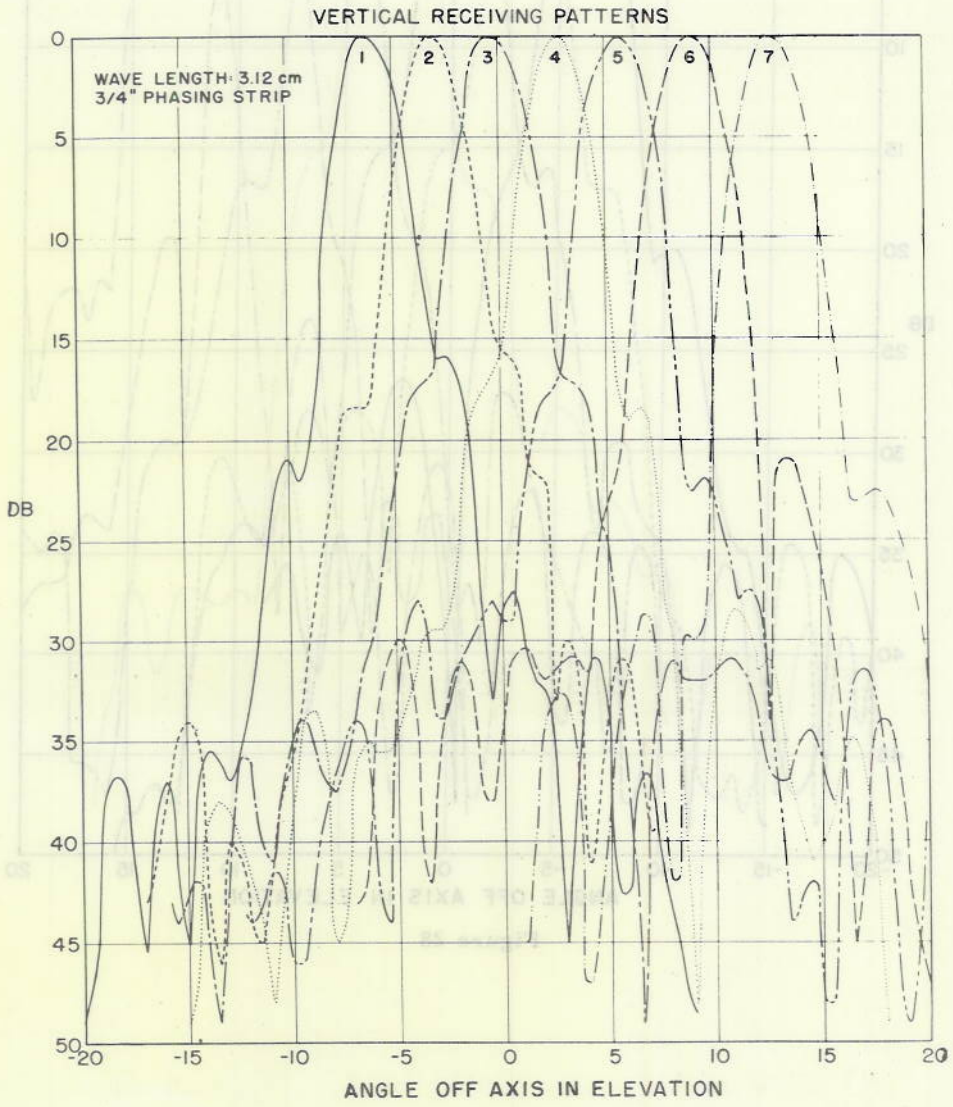


Figure 27

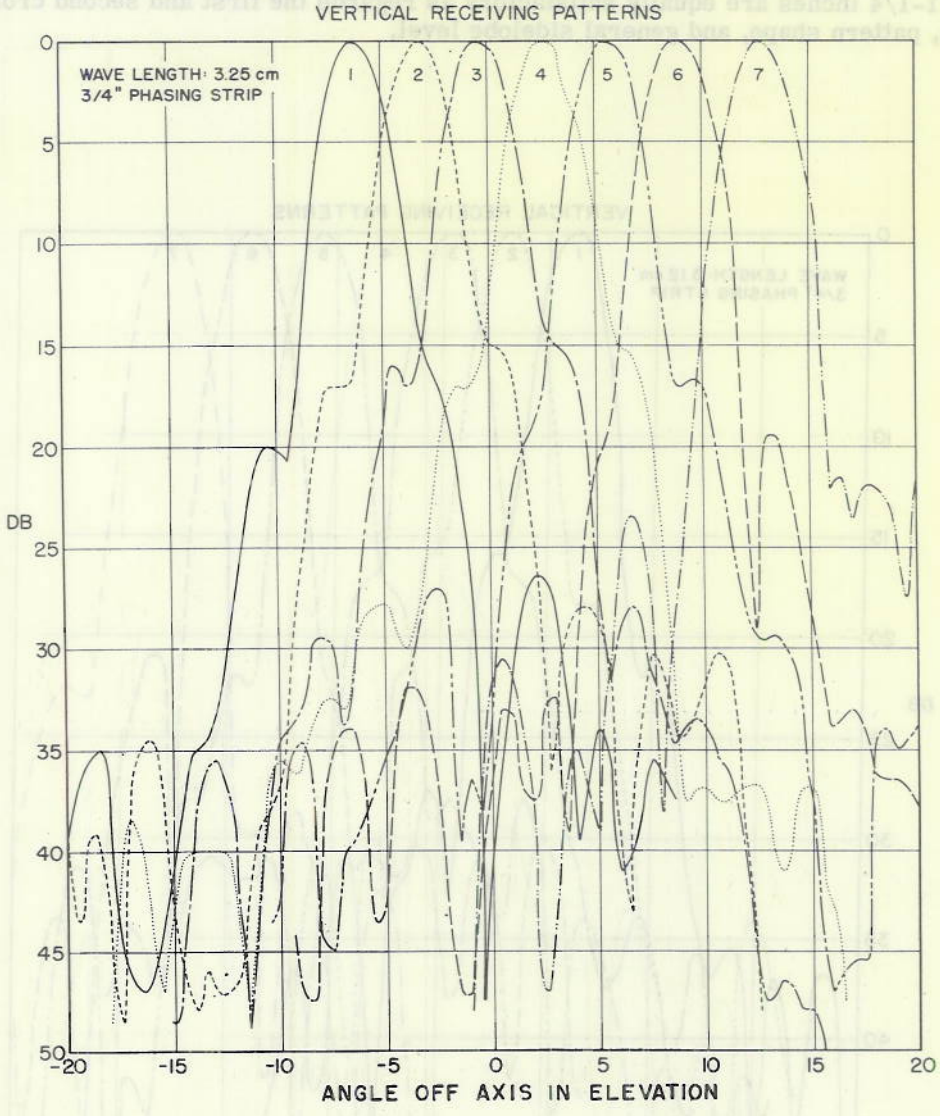


Figure 28

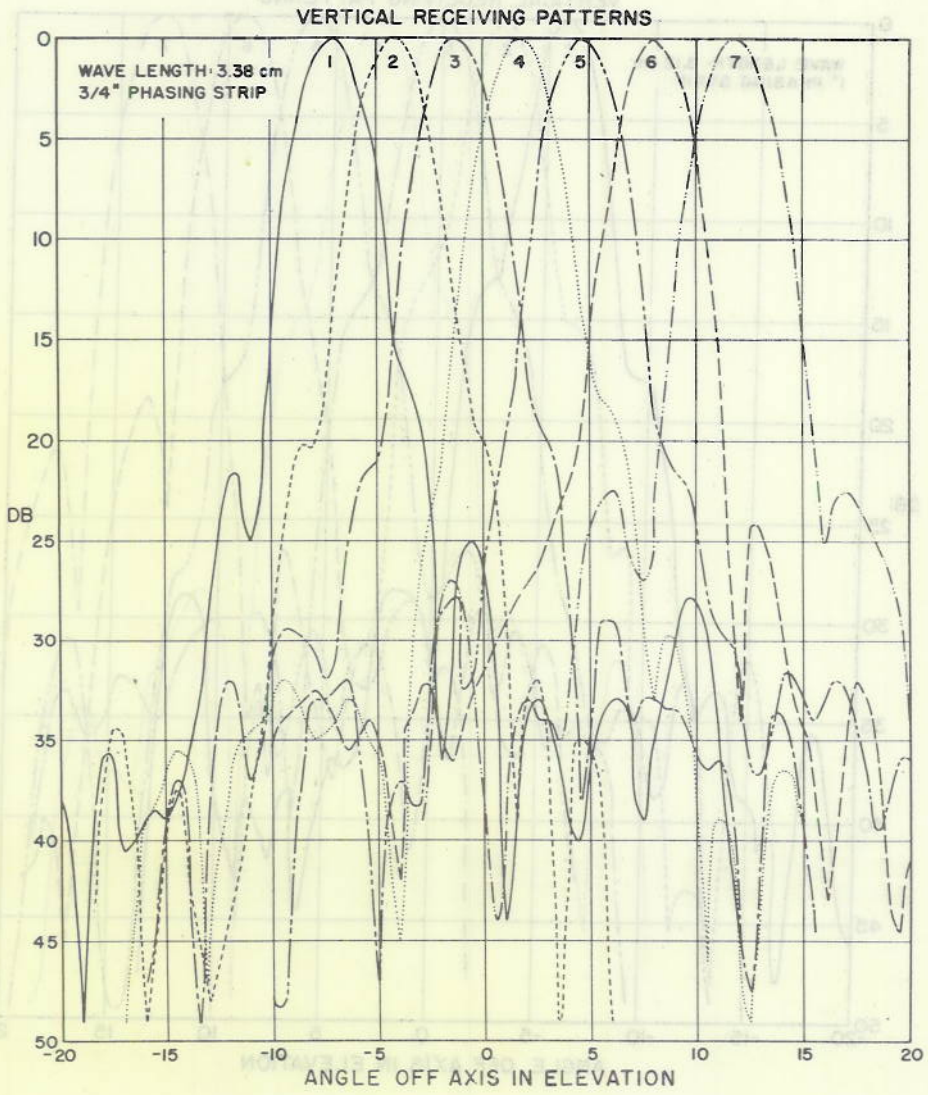


Figure 29

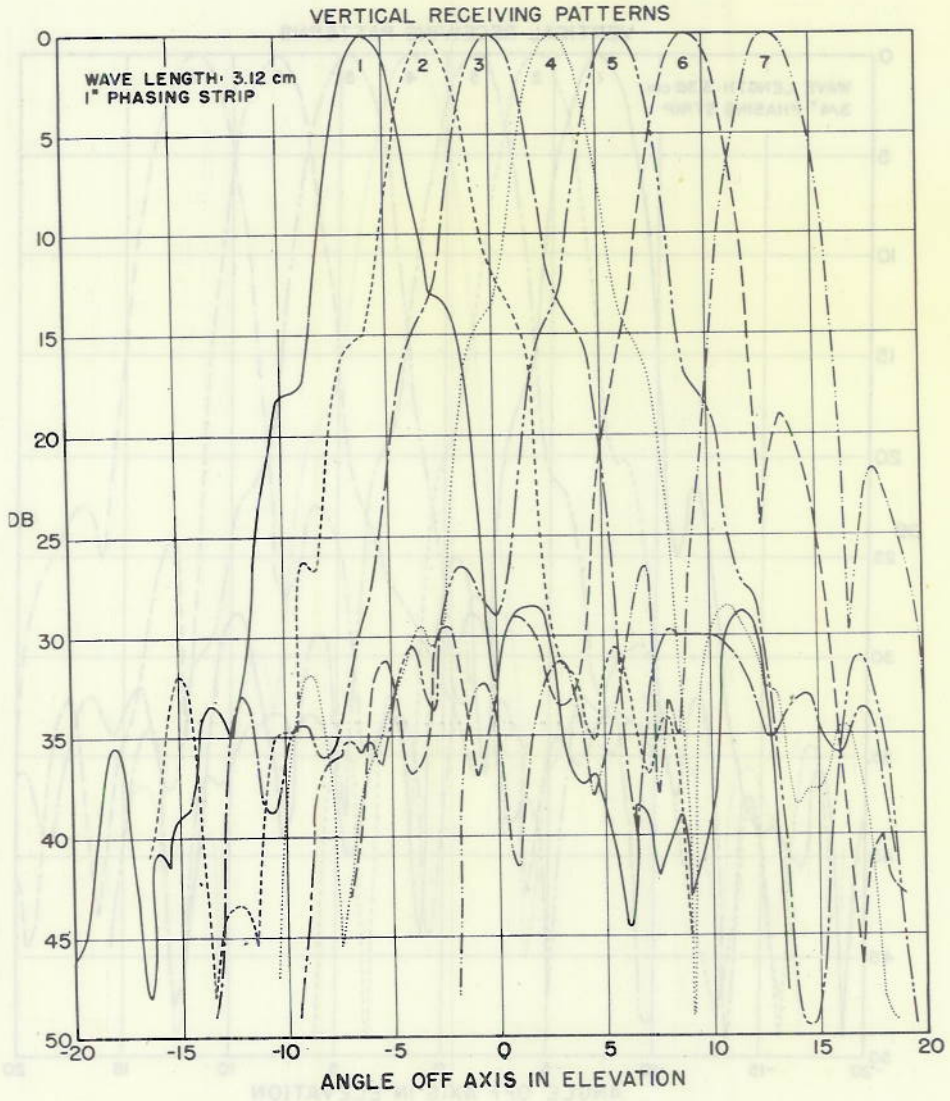


Figure 30

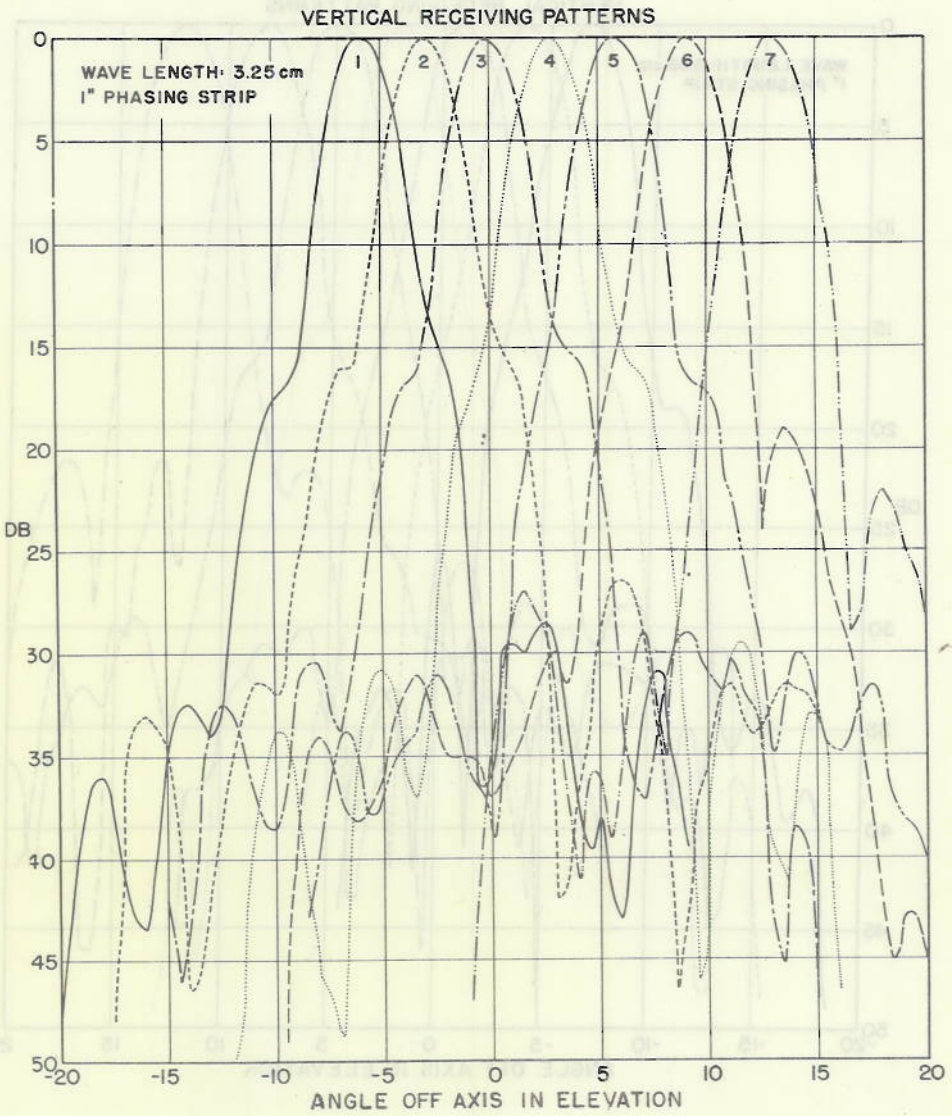


Figure 31

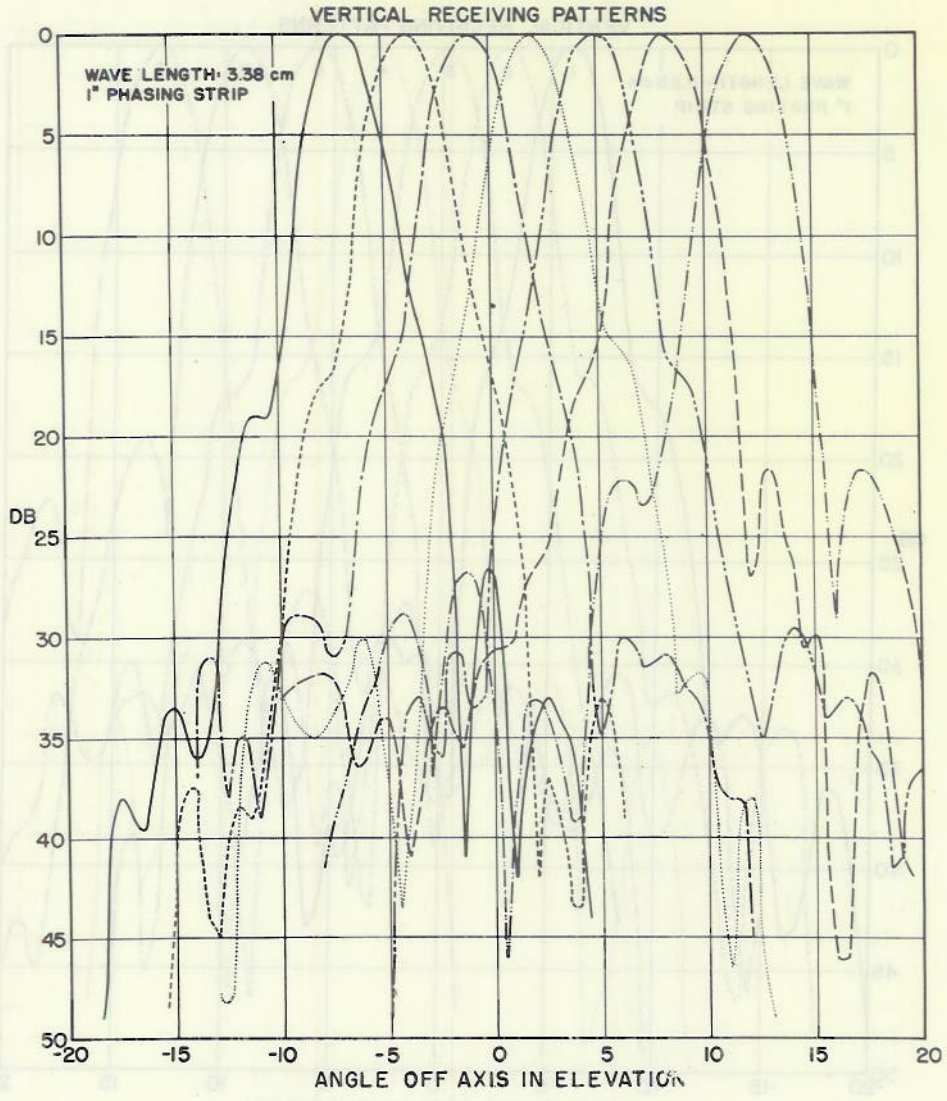


Figure 32

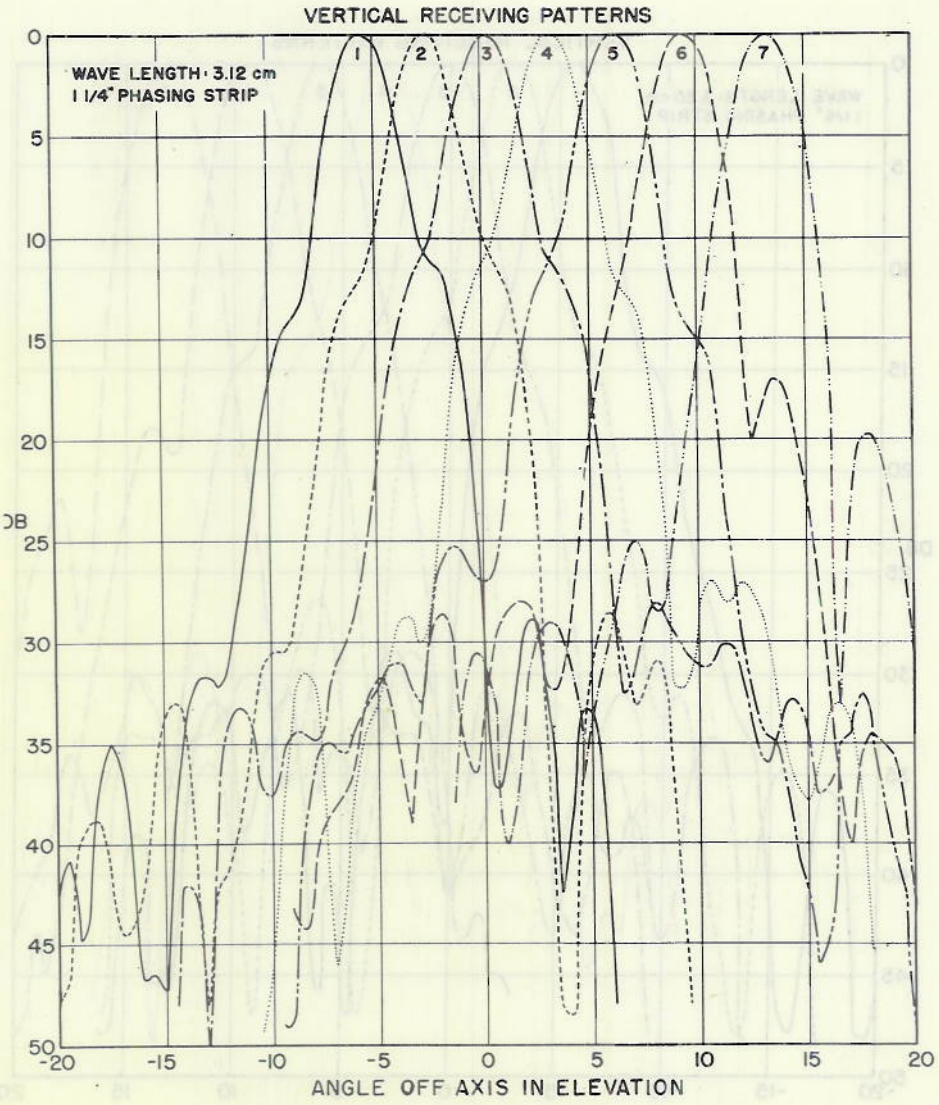


Figure 33

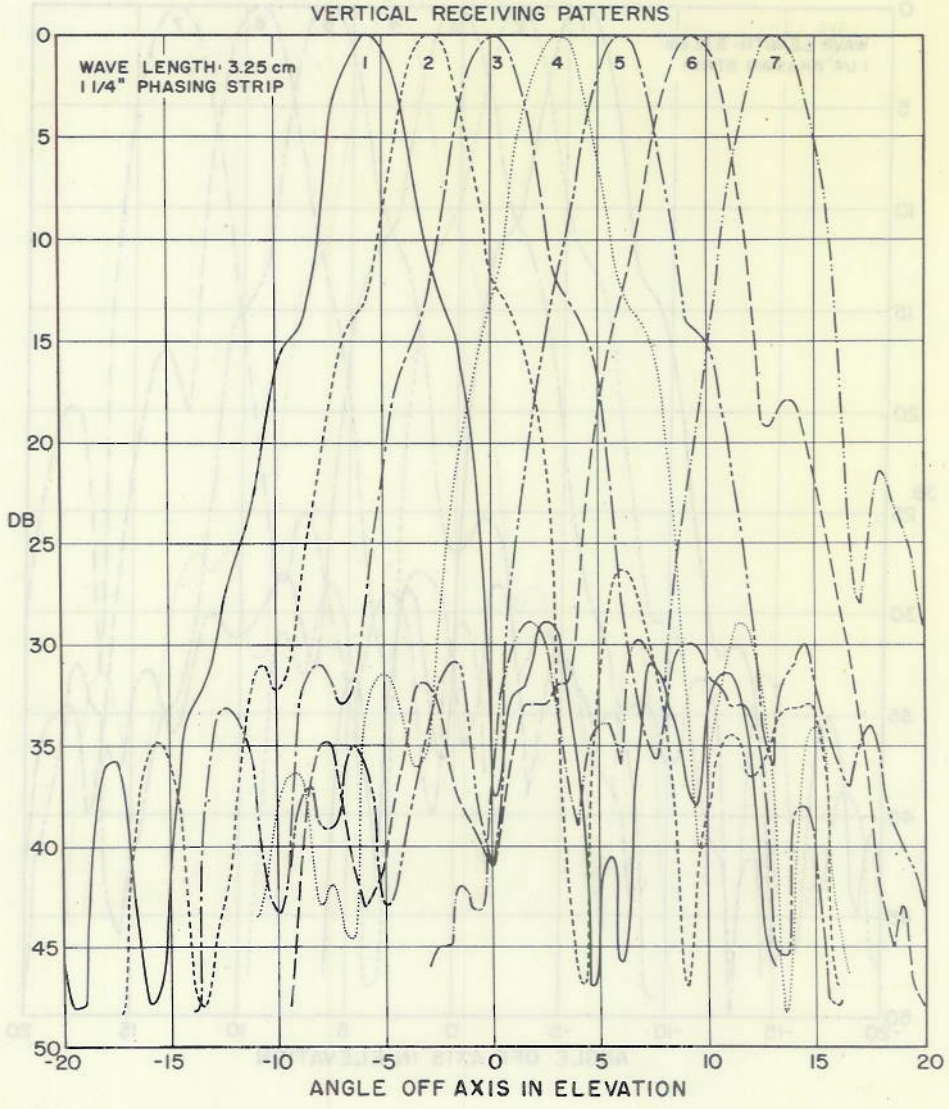


Figure 34

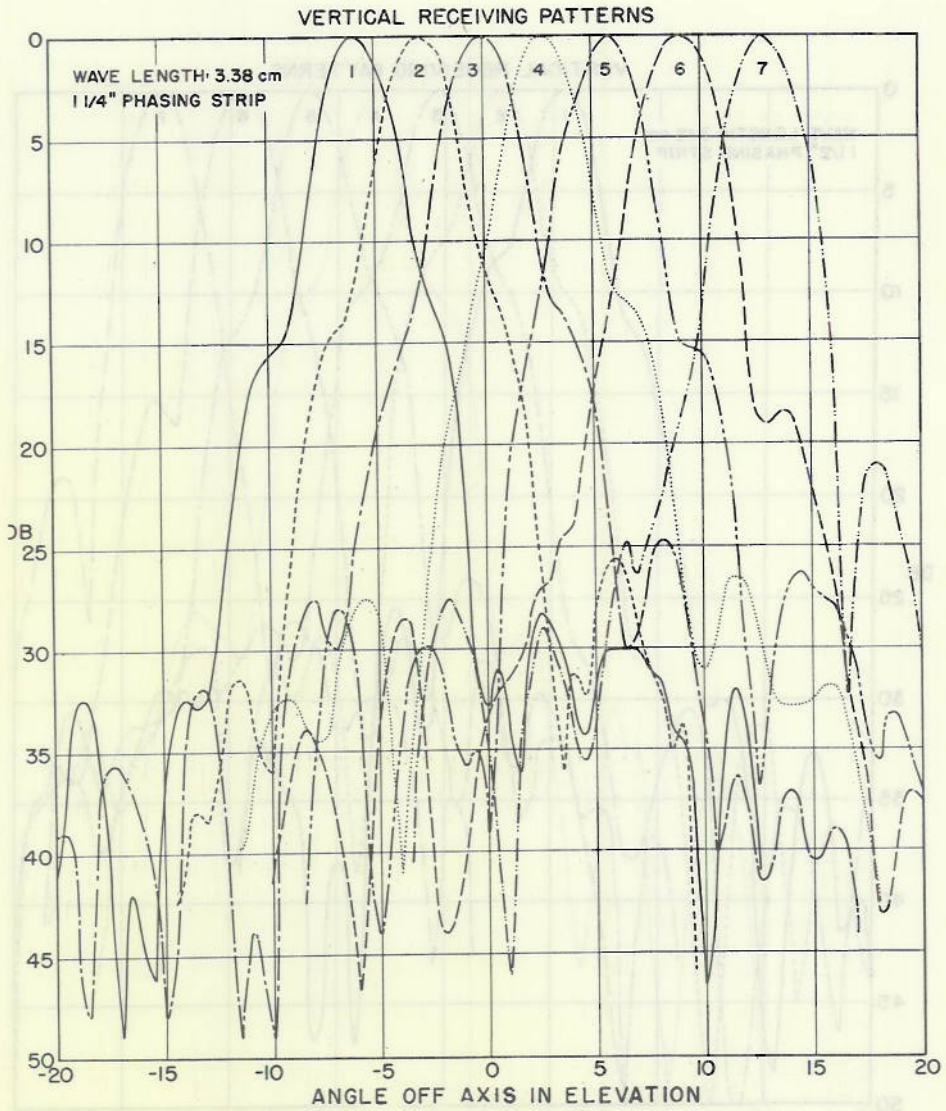


Figure 35

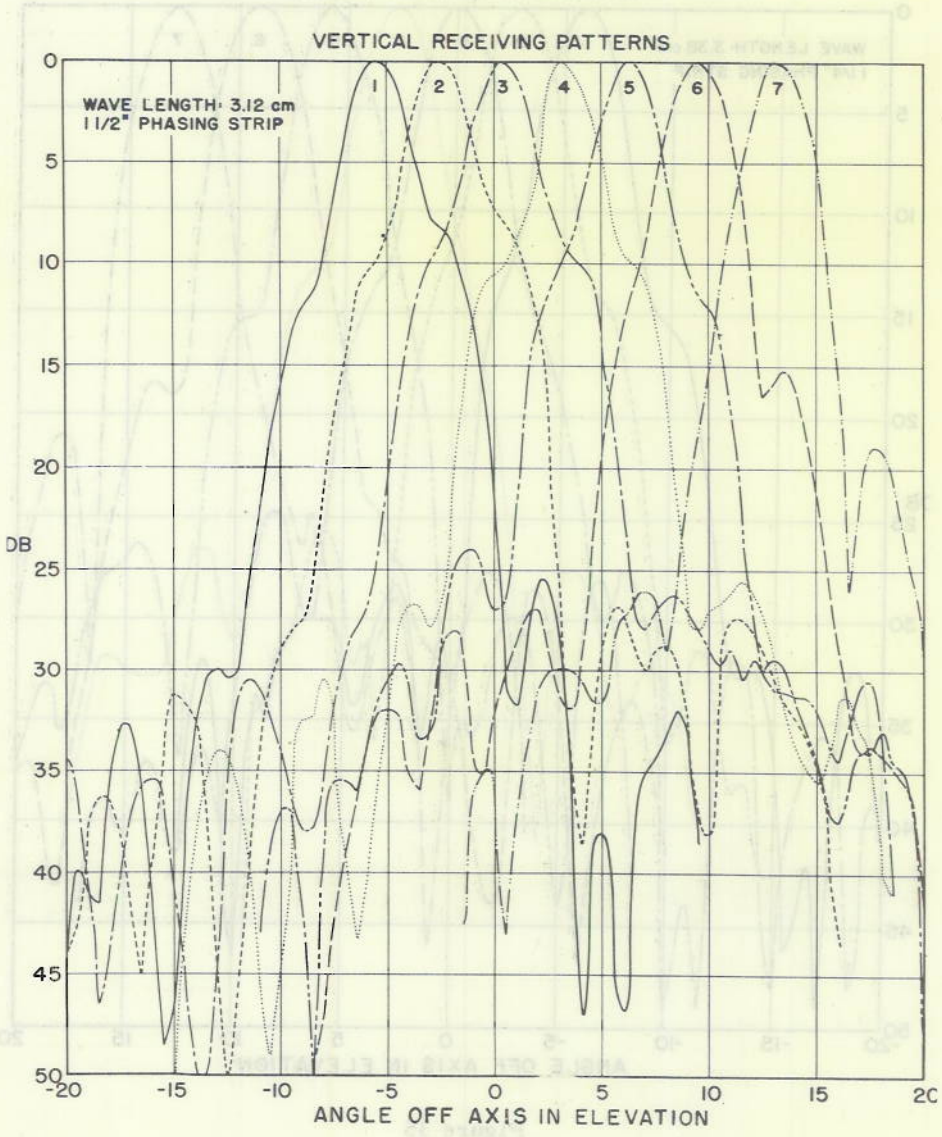


Figure 36

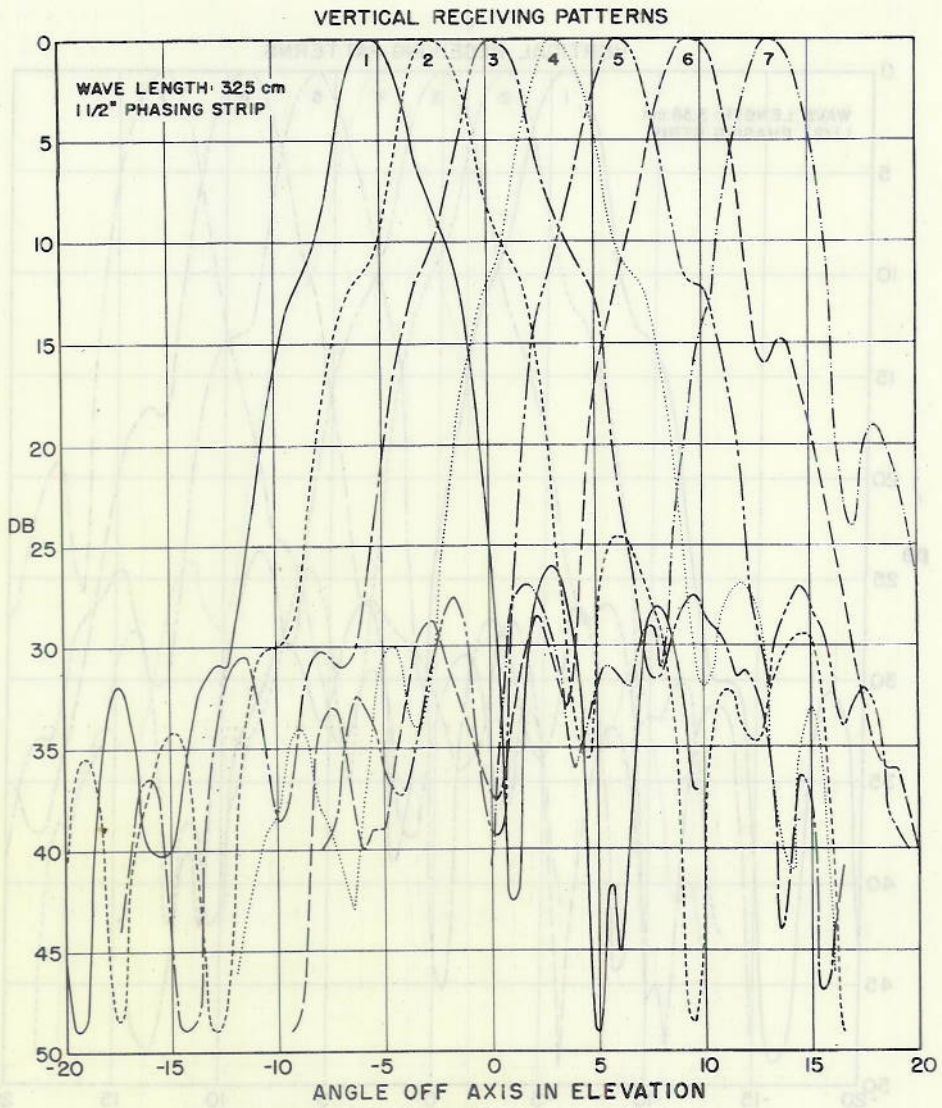


Figure 37

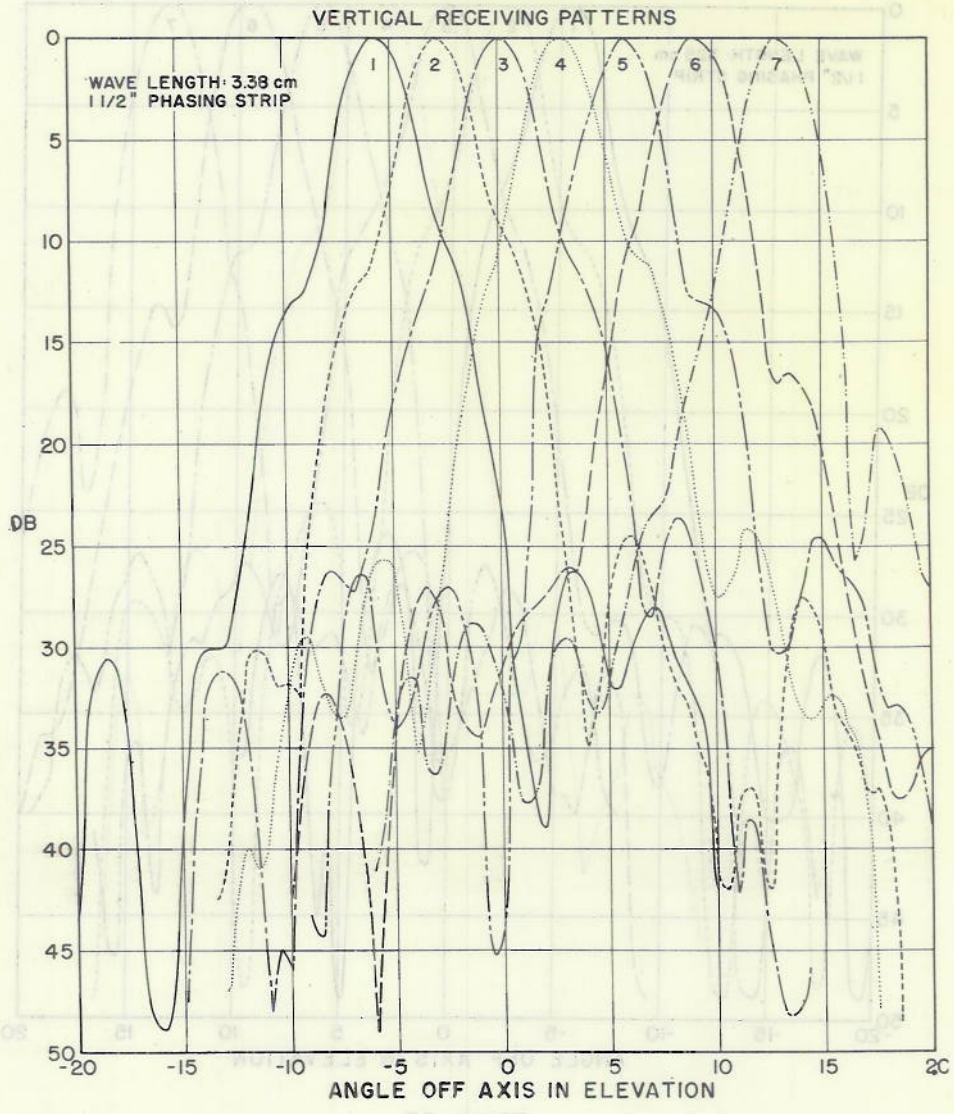


Figure 38

A change of strip height is equivalent to a systematic error in the vertical section of the reflector, which may arise from inaccuracy in construction or from wind distortion. Thus the allowable limits of strip height determine the reflector tolerances. The patterns for 3/4 and 1-1/2 inch phasing strips have second crossovers that are respectively too low and too high. The first defect is the more serious, but the larger strip exhibits a high slidelobe level at the ends of the band which has dictated the adoption of a strip height of $1 \pm 1/4$ inch. The corresponding phase deviation between the center and extremities of the reflector is, from (4),

$$\beta = 71 \pm 18 \text{ degrees} \tag{10}$$

and the reflector tolerance

$$\pm 1/2 \frac{18}{360}\lambda = \pm \frac{9}{40} \text{ in.} = \pm 1/4 \text{ in.} \tag{11}$$

By way of comparison, the tolerance for a single-beam reflector on this wavelength would be approximately $\pm 1/2$ inch.

## Method of Computing Target Height

Height finding is accomplished in the AN/SPS-2 system through a comparison of the video outputs of logarithmic-response receivers associated with each beam. After detection, the signals from adjacent pairs of beams are combined in six "sum" and six "difference" channels. A peak selector chooses the largest sum signal appearing at any given instant, and initiates an impulse whose amplitude is proportional to the crossover angle of this beam-pair. Then an interpolation voltage proportional to the corresponding difference signal, which may be either positive or negative, is added to this pulse to give a measure of elevation angle. The sine of this angle is multiplied by the range to obtain the vertical deflection voltage for a range-height indicator. Intensity modulation proportional to the largest sum signal is provided by the peak selector, which suppresses noise from the other channels.

## Off-Axis Vertical Patterns

As the antenna sweeps through a target in azimuth, six or more significant pulses are received and fed to the height computer. Thus the height accuracy depends on the shape of the vertical patterns either side of the center plane. Ideally, the sum patterns should have a sharp crossover point, independent of azimuth angle. The difference patterns should be linear between beam centers and have fixed slopes. Figures 39 through 42 show sets of vertical patterns taken on the axis and at 2, 3, and 5 db points on the right side of the beams. Corresponding sum patterns are shown in Figures 43 through 46. The progressive shift of the crossover point to higher angles, from figure to figure, results from imperfect alignment of the feed-horn array with the vertical center-line of the reflector, as does the inequality of the positive and negative excursions of the difference curves in Figure 47. The off-axis patterns are being repeated at the present time, and will be the basis of an analysis of height-finding errors to be included in a later report.

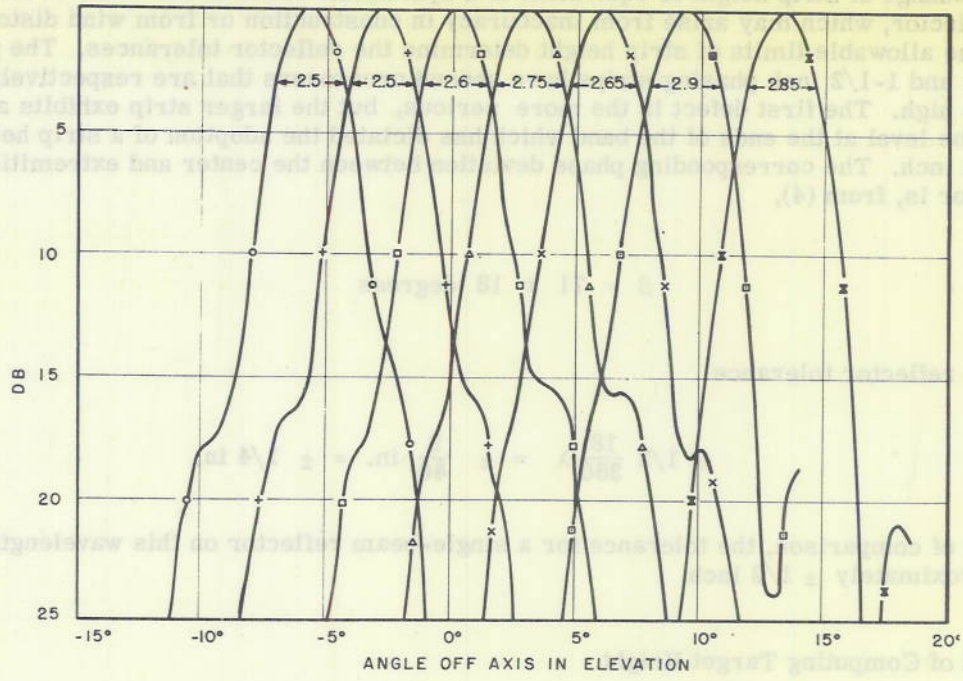


Figure 39 - Vertical patterns on axis at 3.25-cm wavelength, with 1-inch phasing-strip

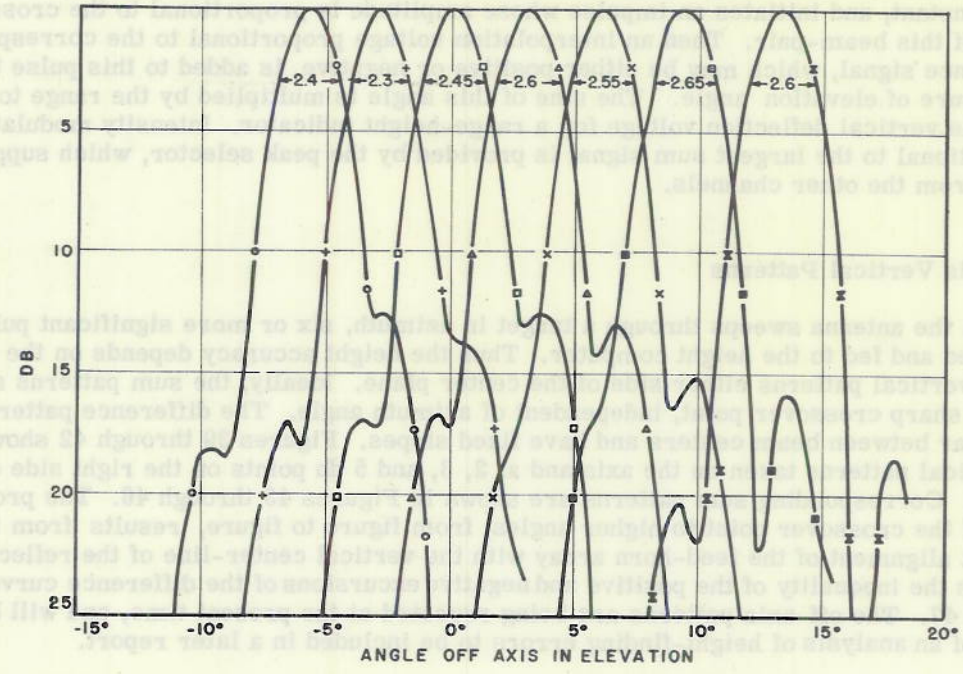


Figure 40 - Vertical patterns at 2-db point on right side of beams

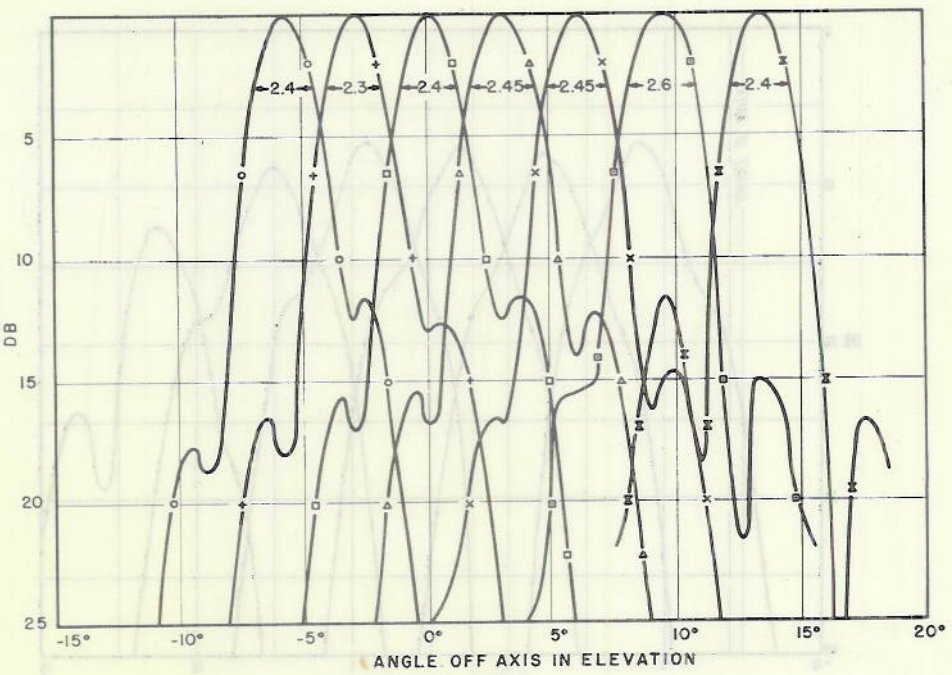


Figure 41 - Vertical patterns at 3-db point on right side of beams

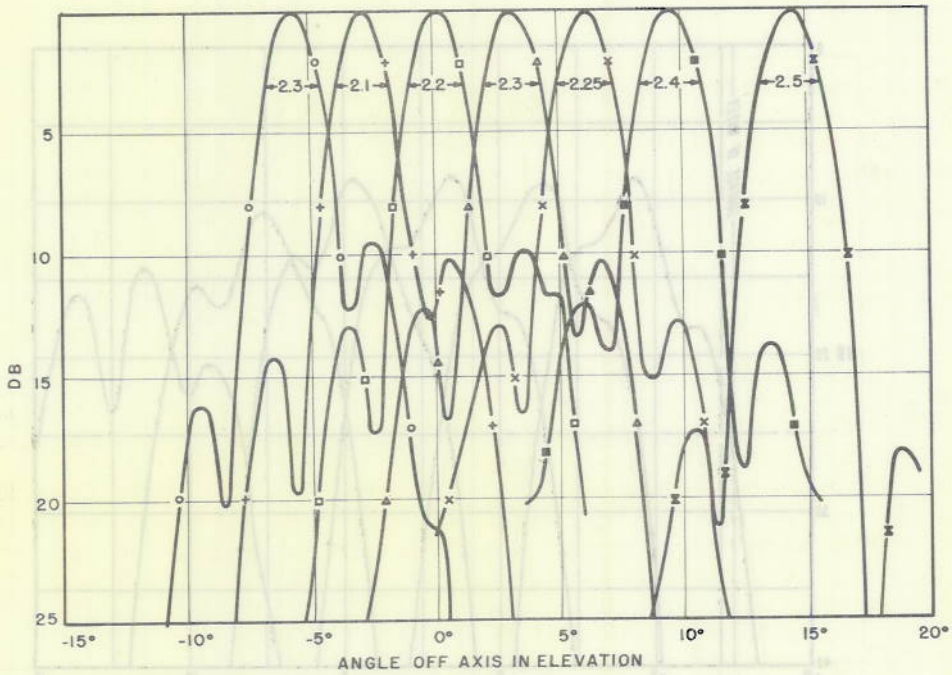


Figure 42 - Vertical patterns at 5-db point on right side of beams

CONFIDENTIAL

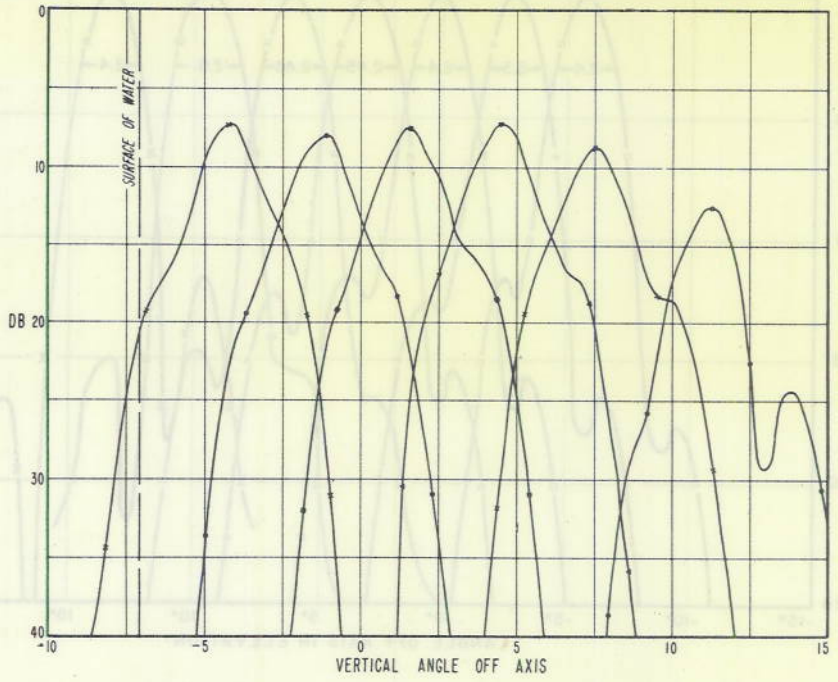


Figure 43 - Vertical sum patterns on axis

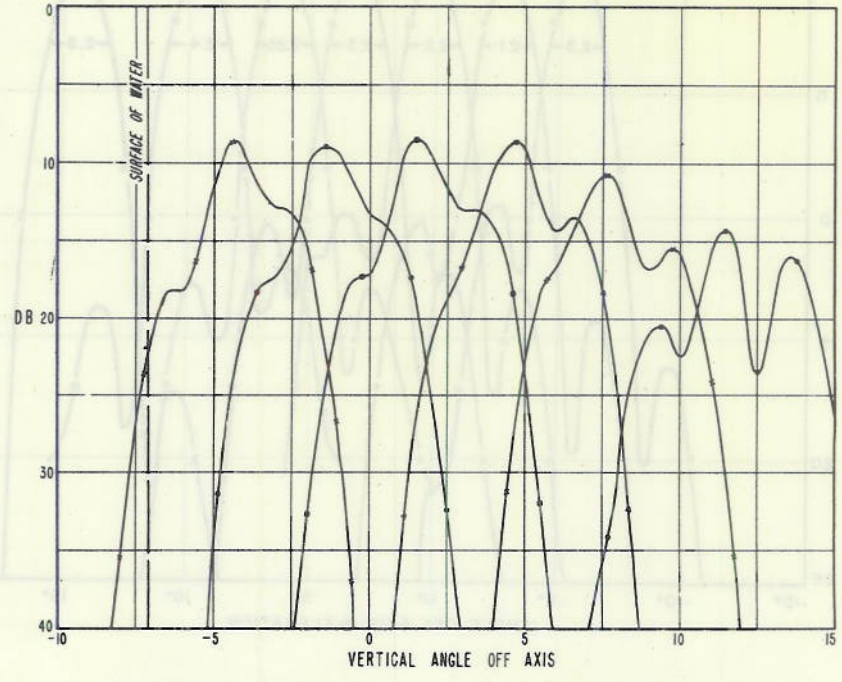


Figure 44 - Vertical sum patterns at 2-db point on right side of beams

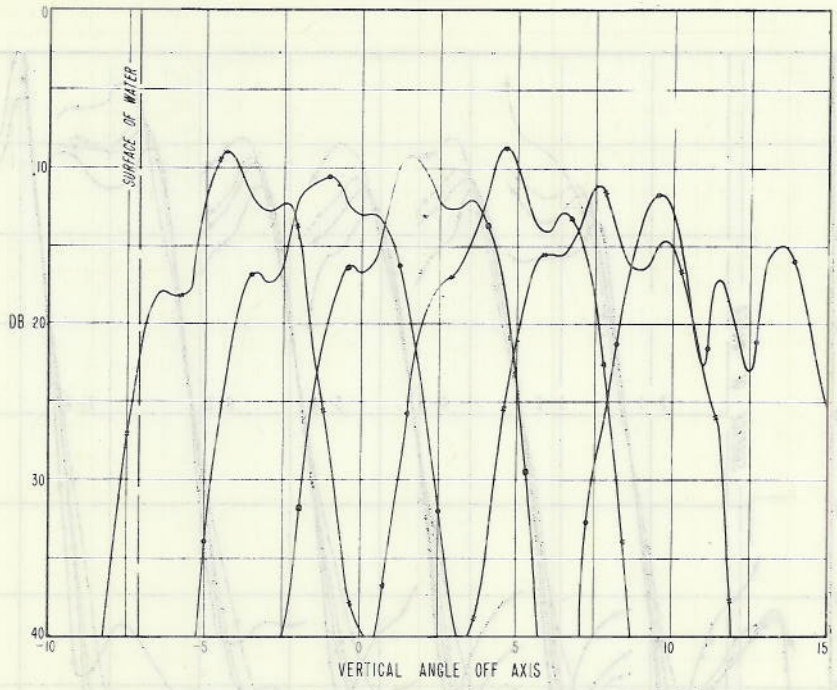


Figure 45 - Vertical sum patterns at 3-db point on right side of beams

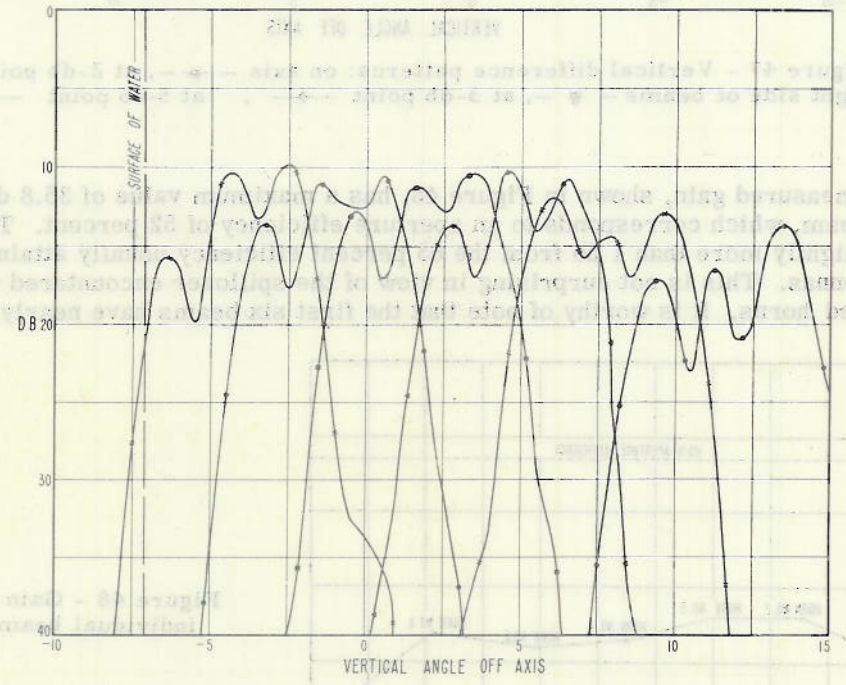


Figure 46 - Vertical sum patterns at 5-db point on right side of beams

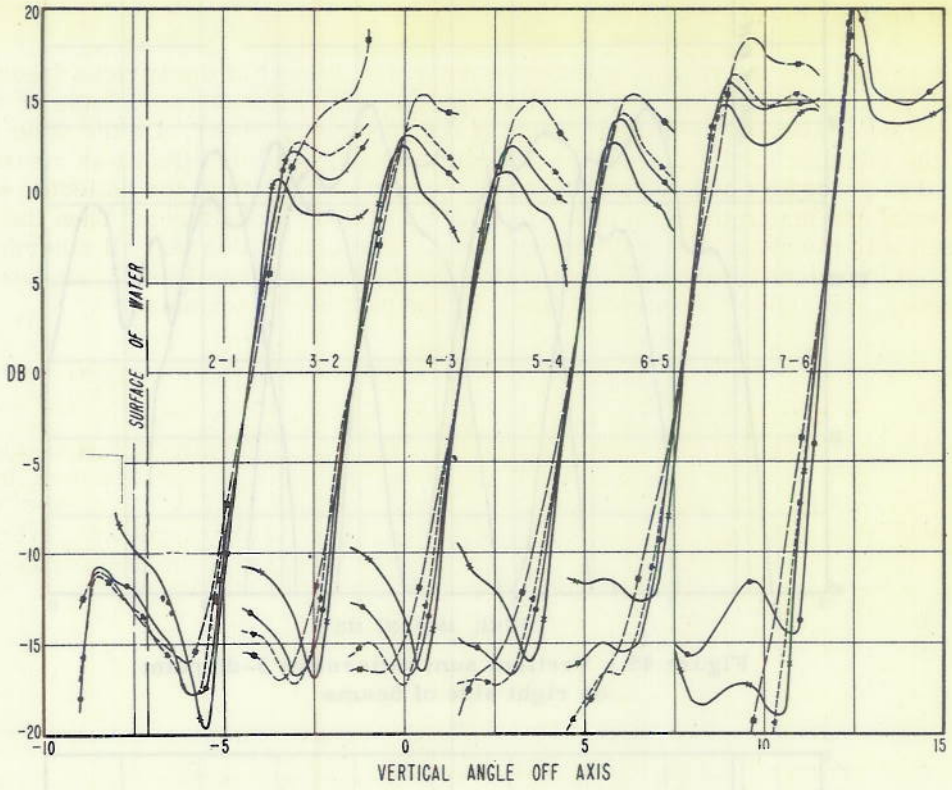


Figure 47 - Vertical difference patterns: on axis — ■ —, at 2-db point on right side of beams — ▼ —, at 3-db point —●— , at 5-db point —✕—

## Gain

The measured gain, shown in Figure 48, has a maximum value of 36.8 db for the on-axis beam, which corresponds to an aperture efficiency of 52 percent. Thus the gain is down slightly more than 1 db from the 65 percent efficiency usually attained in a single-beam antennas. This is not surprising in view of the spillover encountered with the close-spaced feed horns. It is worthy of note that the first six beams have nearly equal gain.

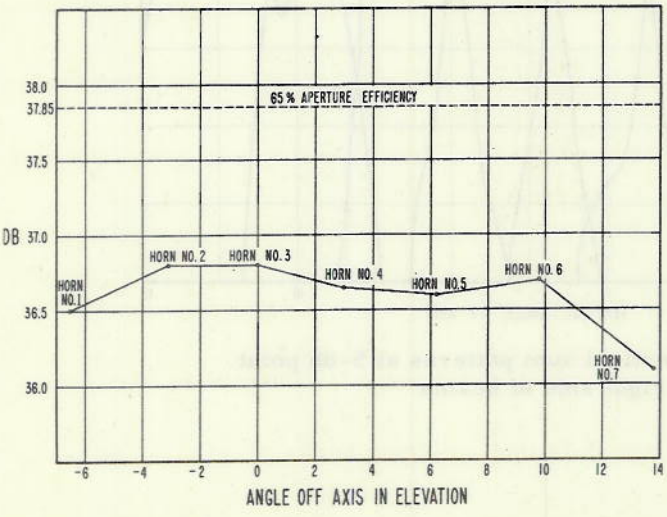


Figure 48 - Gain of the individual beams

Match of the Individual Feed Horns

Figure 49 gives the voltage standing-wave ratio (vswr) of the various feeds across the band, as measured in the reflector through two mitered corners. Some of this mismatch can be eliminated by proper design of a pressurizing cover. On the other hand, that part of the mismatch arising from the reflector cannot, and this effect was measured separately. The procedure adopted was to mask the central portion of the reflector with absorbing material and match the horn under test with a sliding-probe tuner. Then the vswr was measured with the absorbing material removed. Throughout this test all other horns were terminated in matched loads. The reflection coefficient of horns 1 and 3, as determined in this manner, was 0.035. This result was checked against the formula.

$$\left|\Gamma_r\right| = \frac{\lambda g}{4\pi f} \quad . \tag{12}$$

Since the measured value of the gain of No. 3 horn is 10.1, the reflection coefficient from the dish is 0.037, in close agreement with the observed value. It appears then, that the vswr on the individual feed lines cannot be reduced below about 1.08. In view of the difficult problem of matching the power distribution network to the magnetron, every effort should be made to keep this figure as low as possible. Design of the pressurizing cover can best be accomplished in the L-band model.

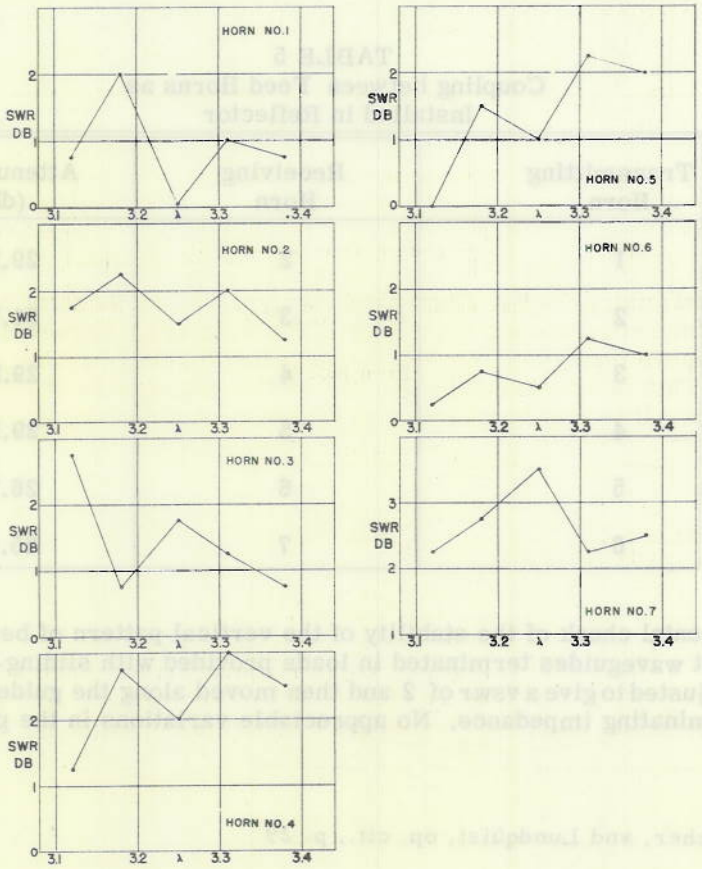


Figure 49 - Match of the individual horns

Coupling

The coupling between adjacent horns is a matter of some concern in a multiple-beam height-finding antenna, since it may distort the shape of the vertical secondary patterns in an unpredictable fashion. This is particularly true in a multiple-frequency radar set, for if part of the energy radiated from horn No. 3, say, is picked up by horns 2 and 4, they will reradiate it without loss of amplitude, but with phases which depend on the exact length of the feed lines. It is reasonable to assume a reflection coefficient magnitude of unity at the magnetrons (or receivers if the TR's are not firing), since the terminal equipment is tuned to another frequency. In designing an antenna for multiple-frequency operation[8] this condition was simulated by terminating the adjacent wave guides with shorting plungers, which were moved through a range of a half guide-wavelength to produce all possible pattern variations. It was found that reasonable pattern stability required a coupling ratio below 30 db.

In the present single-frequency antenna, the individual beams are used only in the receiving condition with each guide matched, at least approximately, to a crystal mixer. If the vswr looking towards the receiver is less than 2, as seems reasonable, the reradiated signal from adjacent horns will be reduced at least 10 db as compared with the case of complete reflection. This means that a coupling ratio of 20 db might be tolerated. However, if the receiver mismatch reaches 4 to 1 as an extreme case, the maximum permissible coupling ratio will be 26 db. The measured values listed in Table 5 just meet the latter requirement. Dish reflections account for the greater part of the coupling, since the observed value of $|\Gamma_r|$ for beams 1 and 3; i.e., 0.035, corresponds to an attenuation of 29.1 db.

TABLE 5
Coupling between Feed Horns as Installed in Reflector

| Transmitting Horn | Receiving Horn | Attenuation (db) |
|---|---|---|
| 1 | 2 | 29.2 |
| 2 | 3 | 31.7 |
| 3 | 4 | 29.2 |
| 4 | 5 | 29.2 |
| 5 | 6 | 26.7 |
| 6 | 7 | 25.8 |

An experimental check of the stability of the vertical pattern of beam No. 3 was made with the adjacent waveguides terminated in loads provided with sliding-probe tuners. The probes were adjusted to give a vswr of 2 and then moved along the guide to vary the phase angle of the terminating impedance. No appreciable variations in the pattern could be detected.

[8] Adams, Kelleher, and Lundquist, op. cit., p. 29

## TRANSMITTING CHARACTERISTICS OF THE ANTENNA

### Power-Division Ratios

In designing a power-dividing network for simultaneous feeding of the seven-horn array, it seemed desirable to make use of hybrid junctions, which have the following advantages: (1) the power division is more nearly independent of load than is the case with E-plane T's and bifurcations, (2) match is more easily achieved, and (3) the input swr is less sensitive to load mismatch. Since devices of this type divide power equally, the fraction of the total energy radiated by any given horn must be expressible as a power of 0.5. The power-division ratios shown in Table 1 meet this requirement, and provide coverage to a uniform altitude of 130,000 feet in all the higher beams, as may be seen by reference to Figure 1. This was desired to assure a high blip/scan ratio on all targets up to 90,000 feet.

### Experimental Power Dividers

The constructional details of an experimental X-band power-division network incorporating hybrid rings are shown in Figures 50 and 51. In addition a second system (Figure 52) using a narrow-face 3-db coupler (Figure 53), designed by H. J. Riblet of Microwave Development Laboratory, has been built and tested. This coupler, since it is of simpler construction than a hybrid ring and permits a more compact design, appears to be preferable from the mechanical standpoint. Accordingly a series of measurements was undertaken to determine the following electrical properties of the two devices: power-division ratio, directivity, input vswr, and power-handling capacity.

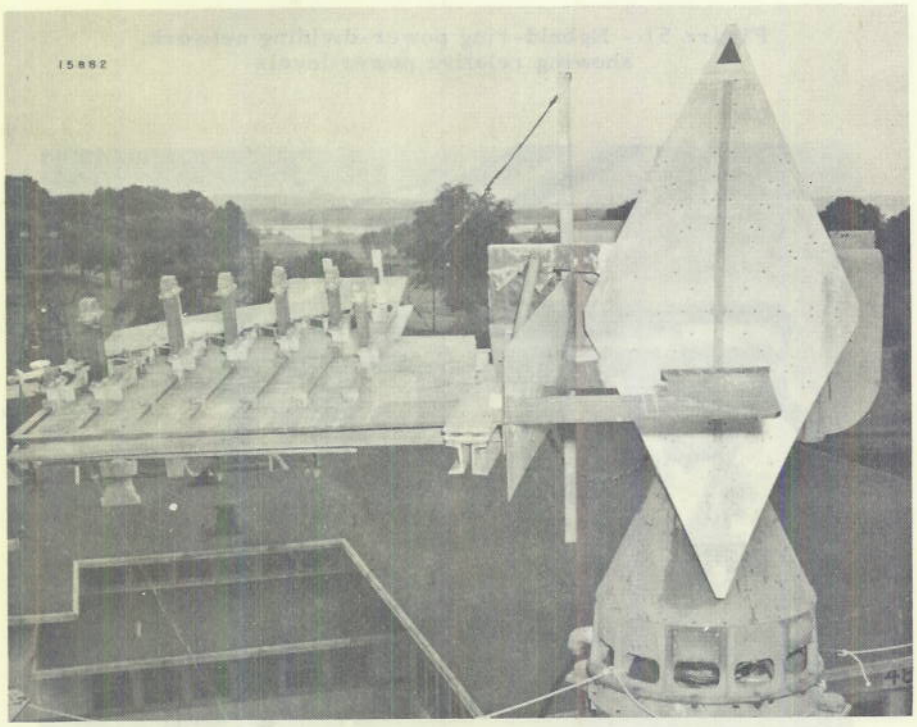


Figure 50 - Antenna in position for vertical transmitting patterns, showing hybrid-ring power-dividing network

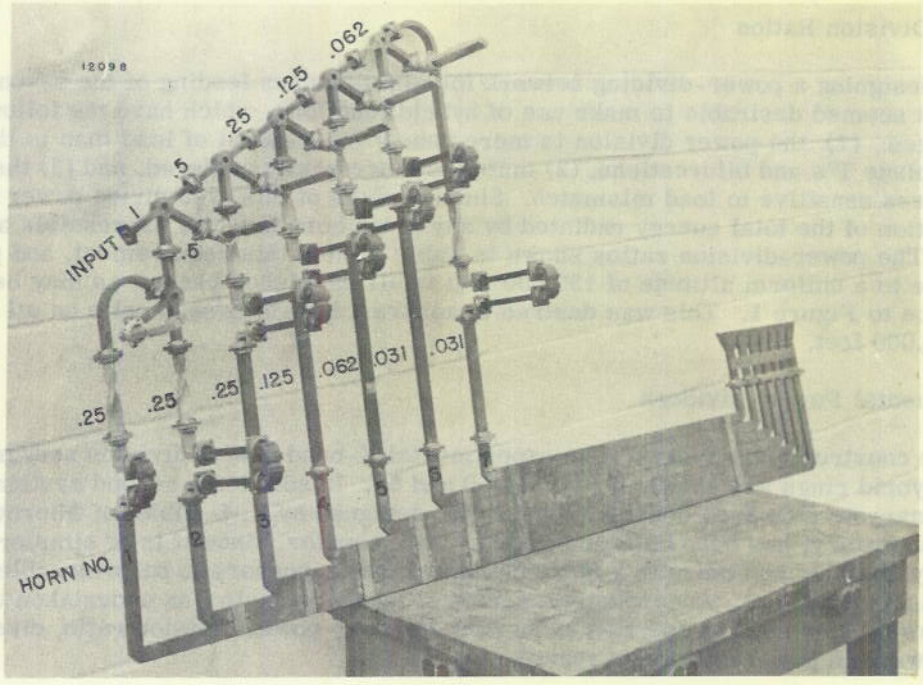


Figure 51 - Hybrid-ring power-dividing network, showing relative power levels

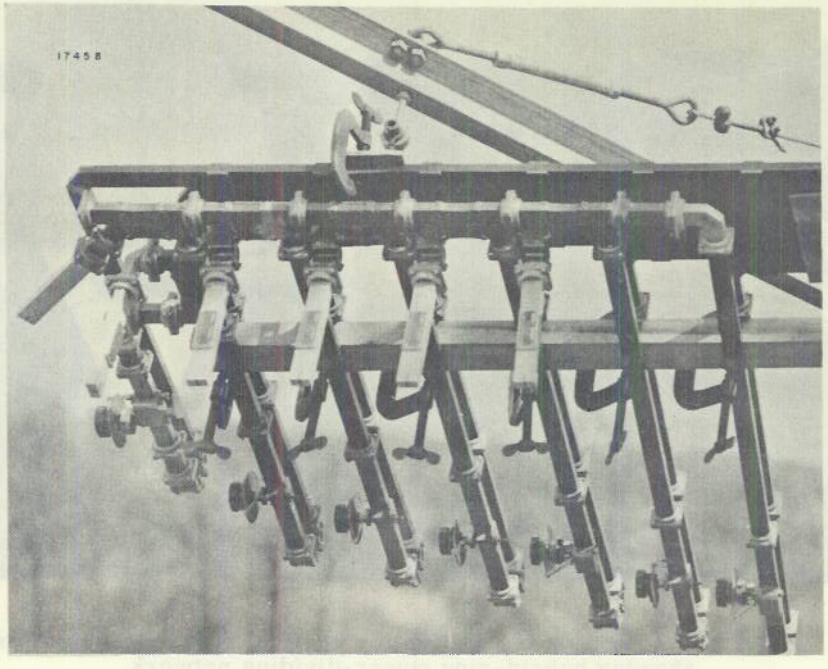


Figure 52 - Riblet-coupler power-dividing network

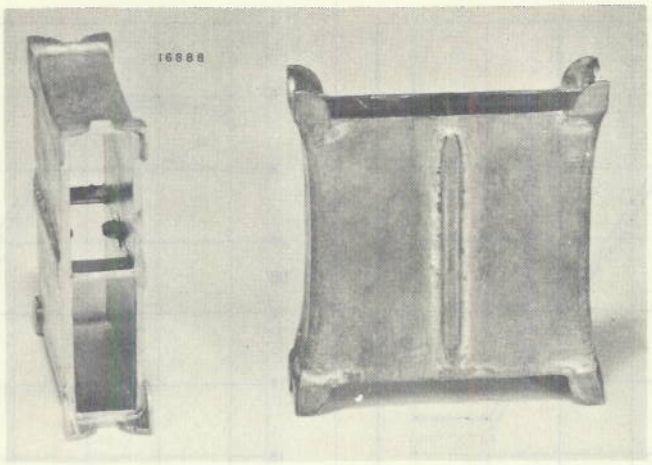


Figure 53 - Three-db directional couplers

Relative Performance of Riblet Couplers and Hybrid Rings

The power level at the two outputs of a Riblet coupler and of a hybrid ring, referred to the input level, is shown as a function of wavelength in Figure 54. Vertical dashed lines represent the edges of an 8-percent band needed for the SPS-2 system. The Riblet coupler seems to have less internal loss than does the hybrid ring; in fact, at some frequencies the total output power appears to exceed the input by as much as 0.3 db. This can only be the result of experimental error. On the other hand, the coupler appears relatively erratic in its power division between the two channels. Its performance in the complete network, however, indicated in Figure 55, is definitely superior to that of the rings in Figure 56. Here the solid line and black points represent the ideal power levels with respect to the input, and the various dashed and dot-dash curves show the observed power division at the center and edges of the band.

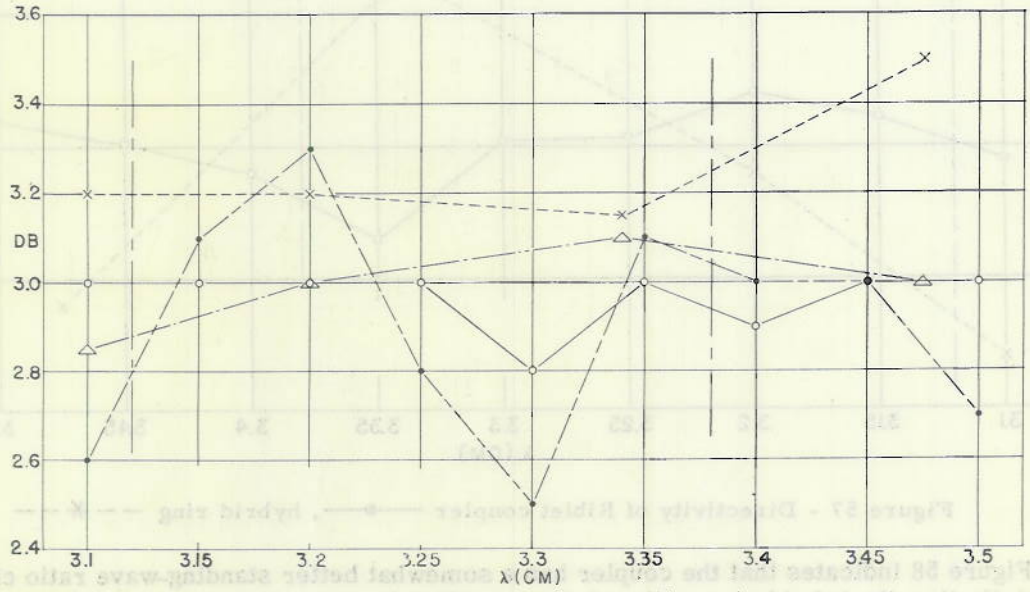


Figure 54 - Observed power output levels. Riblet coupler —o— and – —●— —; Hybrid ring – – – –×– – – – and —·△·—

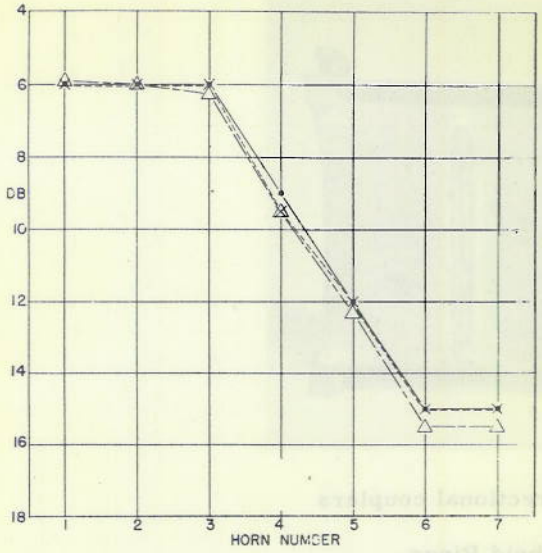


Figure 55 - Relative power supplied to individual channels by Riblet-coupler power-division network: ideal —●—, 3.12 cm —△— —, 3.25 cm – – ✳ – –

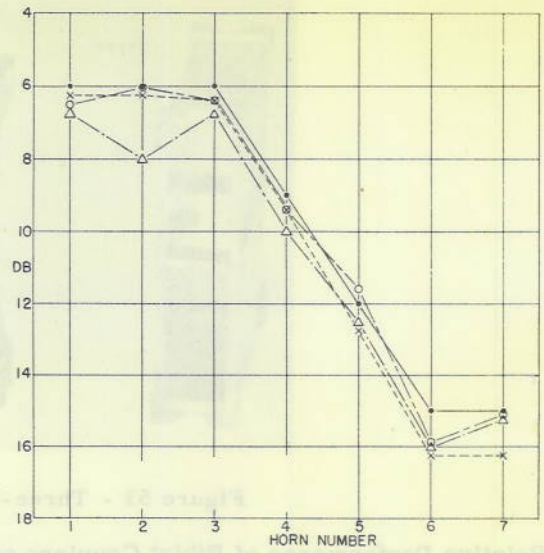


Figure 56 - Relative power supplied to individual channels by hybrid-ring power-division network: ideal —●—, 3.13 cm —△— —, 3.28 cm —✳—, 3.42 cm —○— —

The directivity of the two devices is shown in Figure 57. The hybrid ring attains a high value of directivity at its design frequency, but the coupler exhibits a more uniformly satisfactory behavior over a wide band.

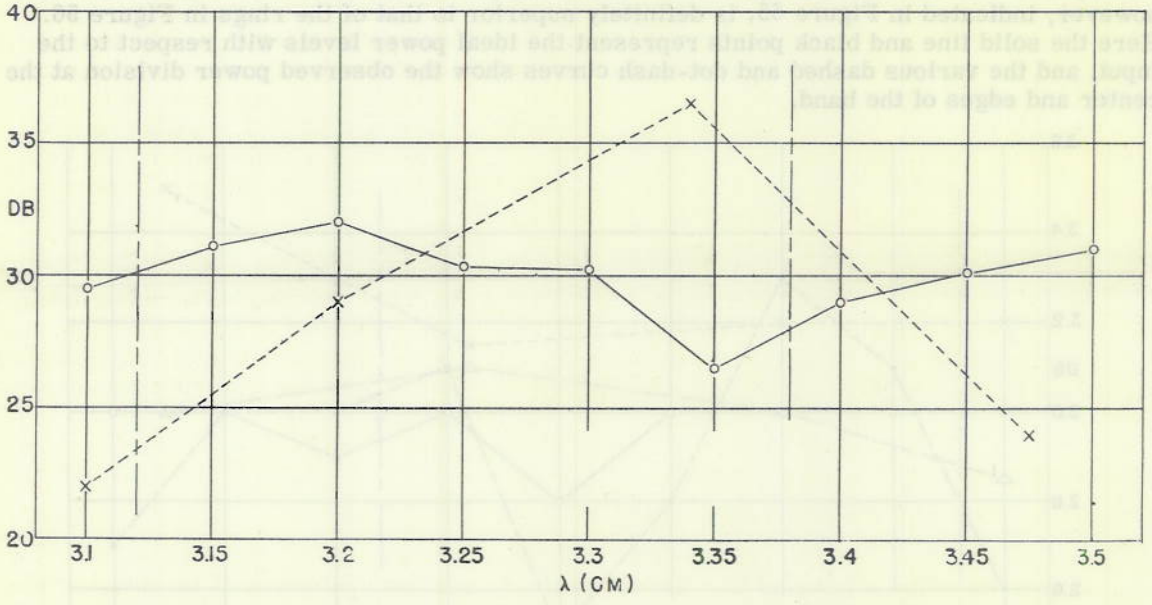


Figure 57 - Directivity of Riblet coupler —○—, hybrid ring – – ✳ – –

Figure 58 indicates that the coupler has a somewhat better standing-wave ratio characteristic than the hybrid ring, although the specified frequency band is not optimum for either device.

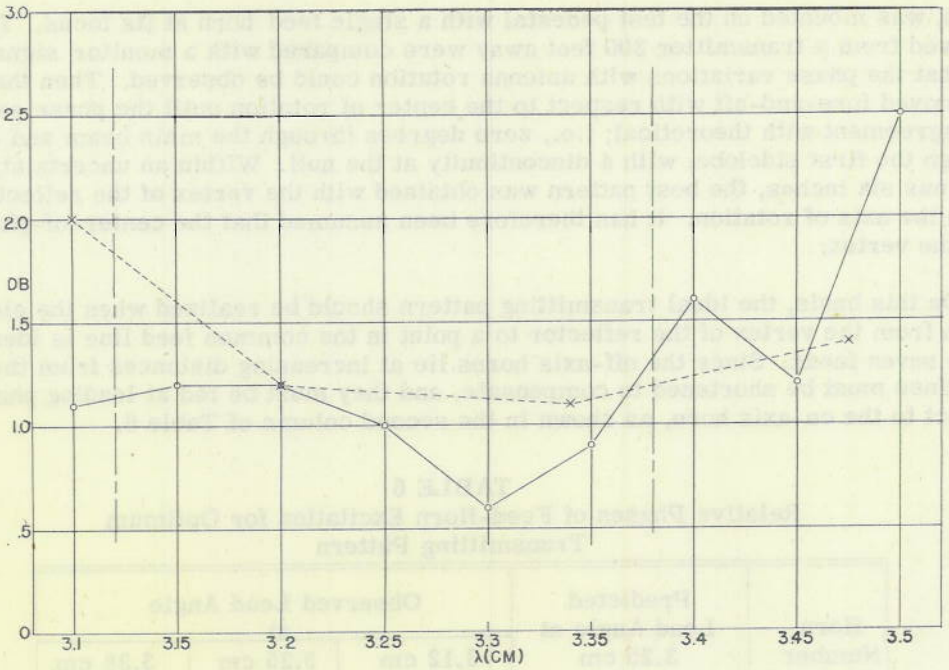


Figure 58 - Standing-wave ratio at input to Riblet coupler —o—, hybrid ring — — — —

Voltage breakdown tests were made with a 4J50 magnetron, at 3.2 centimeters and 0.0015 duty cycle, on two early types of Riblet couplers and a carefully constructed hybrid ring. The couplers had different capacitive loading tabs at the center of the slot—semi-circular in one case, and rectangular (Figure 53, left) in the other—and broke down at 47- and 73-kw peak-power respectively. These values correspond to 2.3 and 3.6 megw at 1300 Mc. The hybrid ring was free of corona at the highest available power, 113 kw, which corresponds to 5.5 megw at 1300 Mc. This result led to the adoption of a hybrid-ring power-dividing network in the fall of 1949.

More recently Dr. Riblet has improved the capabilities of his coupler by substituting flat buttons for the loading tabs, and an L-band version will be used in the production models of the SPS-2 radar. It is quite possible that the superior r-f performance of these couplers will result in a substantial improvement in the transmitting patterns and input standing-wave ratio.

## Simplified Theory of Feed-Horn Phasing

It is reasonable to assume that the optimum transmitting pattern will be obtained when the peaks of the individual beams are in phase, but if this criterion is to be used as a guide in phasing the feed horns, the center-of-phase for secondary patterns must be known. The approximate location of the phase center was determined in the following manner. A paraboloidal reflector of elliptical contour, having about the same dimensions as the AN/SPS-2

model, was mounted on the test pedestal with a single feed horn at its focus. The signals received from a transmitter 300 feet away were compared with a monitor signal in such a way that the phase variations with antenna rotation could be observed. Then the antenna was moved fore-and-aft with respect to the center of rotation until the phase pattern was in best agreement with theoretical; i.e., zero degrees through the main beam and 180 degrees through the first sidelobe, with a discontinuity at the null. Within an uncertainty of plus or minus six inches, the best pattern was obtained with the vertex of the reflector directly above the axis of rotation. It has therefore been assumed that the center-of-phase coincides with the vertex.

On this basis, the ideal transmitting pattern should be realized when the electrical path length from the vertex of the reflector to a point in the common feed line is identical for each of the seven feeds. Since the off-axis horns lie at increasing distances from the vertex, their feed lines must be shortened to compensate, and they must be fed at leading phase angles with respect to the on-axis horn, as shown in the second column of Table 6.

TABLE 6
Relative Phases of Feed-Horn Excitation for Optimum Transmitting Pattern

| Horn Number | Predicted Lead Angle at 3.25 cm | Observed Lead Angle at | | |
|---|---|---|---|---|
| | | 3.12 cm | 3.25 cm | 3.38 cm |
| 1 | 48° | 34° | 39° | 47° |
| 2 | 12 | 9 | 7 | 9 |
| 3 | 0 | 0 | 0 | 0 |
| 4 | 12 | 62 | 72 | 62 |
| 5 | 48 | 166 | 162 | 163 |
| 6 | 119 | 291 | 273 | 263 |
| 7 | 236 | 366 | 330 | 308 |

### Procedure for Phasing the Feed Horns

In order to avoid the frequency-sensitivity that would result from accidental inclusion of one or more extra wavelengths of guide in any of the feed lines, these lines were set equal, within the error of physical measurement, by adjusting the hairpin sections visible in Figures 50 and 51. Then seven calibrated phase-shifters of equal length were inserted into the power-dividing network and varied to obtain the best possible transmitting pattern. Figure 59 is a photograph of one of these phase-shifters with the two end sections of guide removed. The dielectric strip is long enough to furnish more than 360 degrees of phase shift. When a satisfactory pattern had been obtained, the phase-shifters were removed and the hairpin sections were cut, in accordance with the observed settings, to restore the phase distribution. Finally the relative phase angles at the horn apertures were measured, at the center and edges of the frequency band, with the results seen in the last three columns of Table 6.

Agreement with the simple theory outlined above is rather good for the first three horns, but there are large deviations for the others. The explanation may lie in the implicit

assumption that each beam can be regarded as adding to the pattern independently of its neighbors. This seems to be justified where the horns are excited equally, but does not hold for any horn adjacent to another carrying more power than it does. Perhaps the large lead angles observed on the higher beams are required to compensate the smaller angles of the strong field contributed by the next lower beam. The situation is complicated by the fact that the phase-gabling across the reflector aperture produces a continuous phase variation throughout the individual beams. This phase pattern will be calculated as well as measured in the near future, for it must be known to predict the height-finding performance of the set at small elevation angles, where water reflection sets up interference lobes. It will then be possible to understand the synthesis of the transmitting pattern in greater detail.

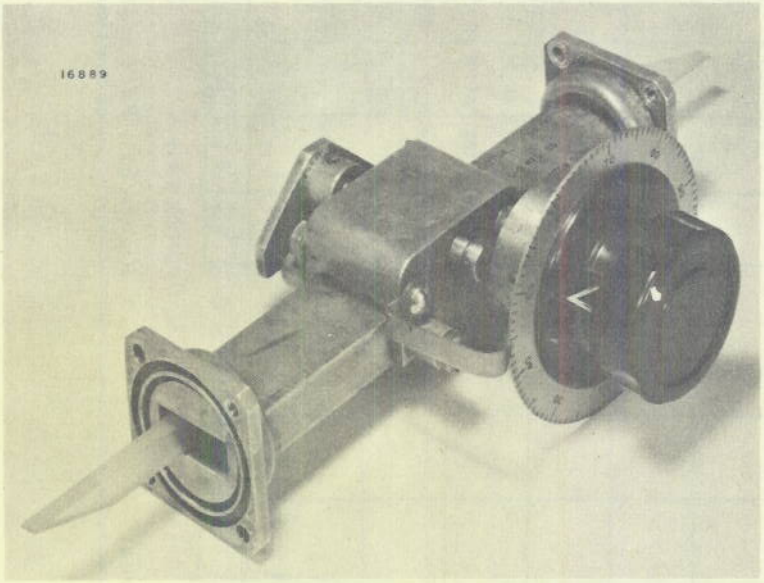


Figure 59 - Calibrated variable phase-shifter

Vertical Transmitting Patterns

Vertical transmitting patterns are shown in Figure 60 for the center and two ends of the frequency band. As a result of the care taken to maintain equal path lengths for the individual feed lines, the pattern shape is nearly independent of frequency.

Transmitting Contours

Free-space contours of the transmitting pattern are plotted in Figure 61. It will be noted that the region between 5 and 10 degrees off-axis in azimuth and between the horizon and 10 degrees elevation contains several lobes only 25 db down from peak intensity. Fortunately, as may be seen in Figure 62, these lobes are greatly reduced by the effects of reflection from the surface of the water; a similar effect was noted in the receiving patterns of the lower beams. The contours of Figure 62 were derived from Figure 61 by adding field strengths at corresponding points above and below the horizon, and thus represent the interference maxima.

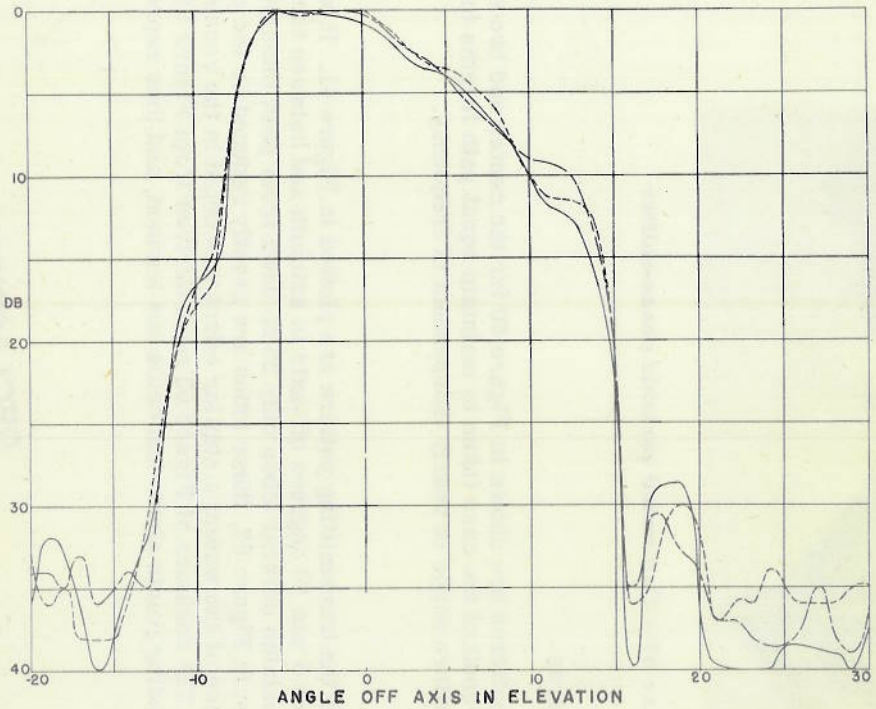


Figure 60 - Vertical transmitting patterns:
3.14 cm — - —, 3.25 ———, 3.38 cm -------

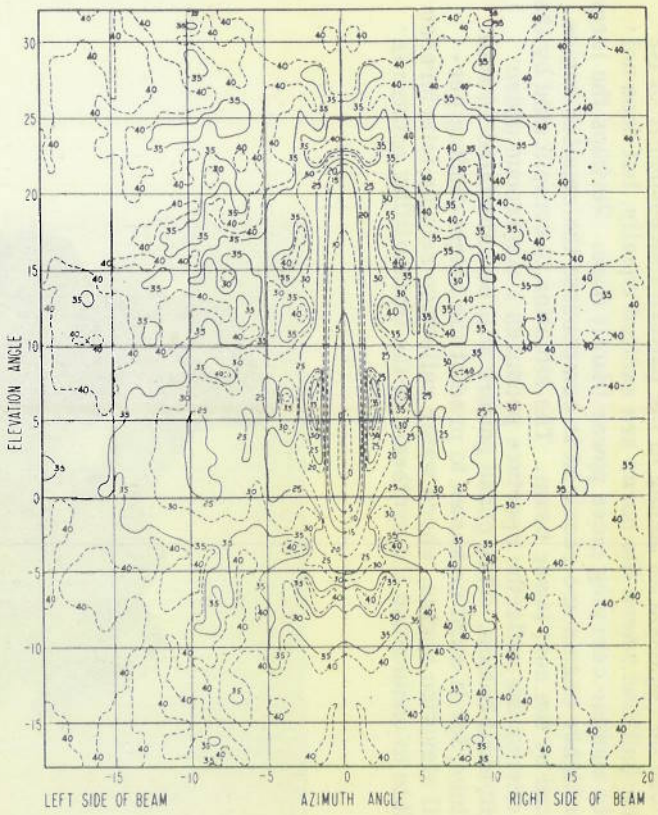


Figure 61 - Free space equal-intensity contours of the transmitting beam

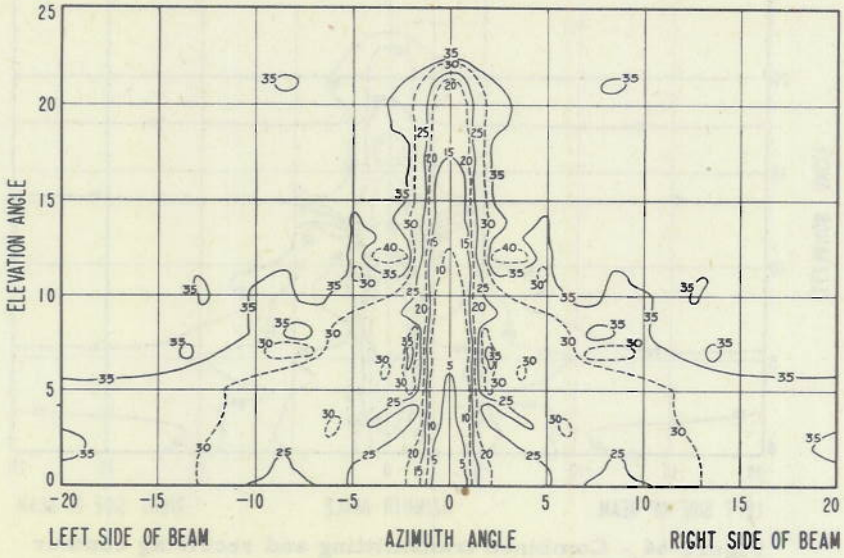


Figure 62 - Equal-intensity contours of the transmitting beam after correction for reflection from the water

## Combined Transmitting and Receiving Contours

The corrected transmitting and receiving contours were added point by point in db to obtain the composite curves shown in Figures 63, 64, and 65. The peak intensity was adjusted to zero db in each case. These are round-trip intensity contours, and give a graphical picture of the resolution of the radar. The lower beams are relatively clean, but No. 7 displays a series of high lobes in the vertical plane, which arise from the taper of the transmitting pattern.

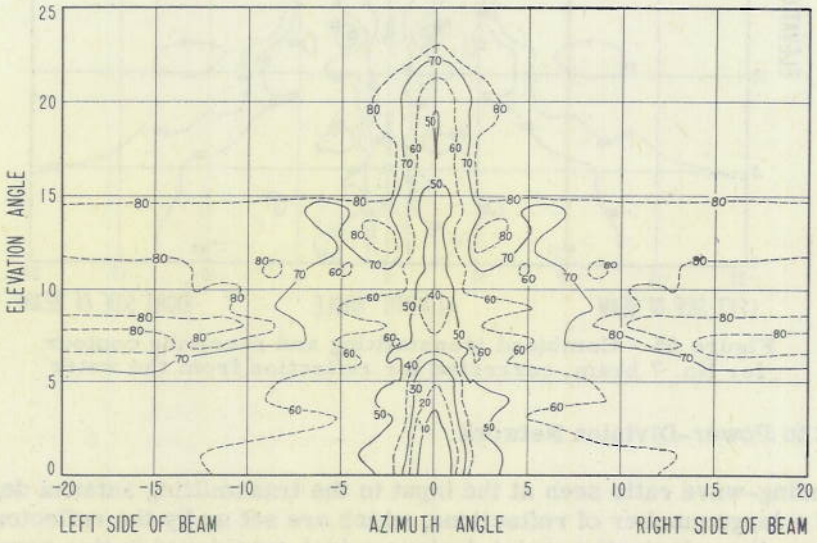


Figure 63 - Combined transmitting and receiving contour for No. 1 beam, corrected for reflection from the water

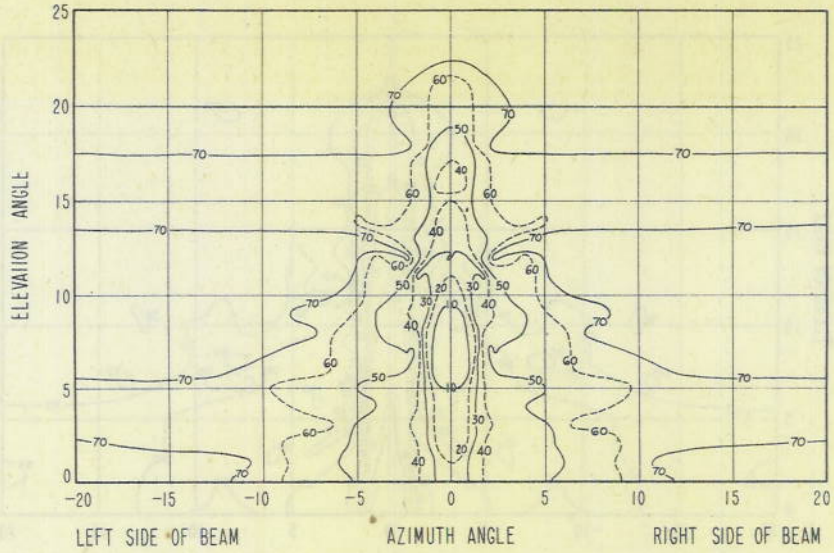


Figure 64 - Combined transmitting and receiving contour for No. 3 beam, corrected for reflection from the water

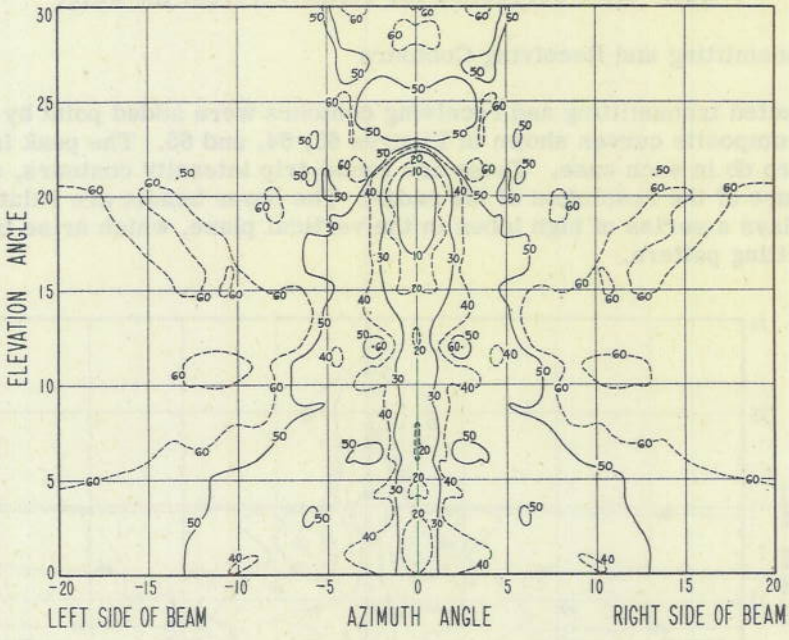


Figure 65 - Combined transmitting and receiving contour for No. 7 beam, corrected for reflection from the water

## SWR at Input to Power-Division Network

The standing-wave ratio seen at the input to the transmitting antenna depends on the magnitude of a large number of reflections, which are set up by the reflector itself, the horn apertures, the polarization-twist duplexers (not considered in this report), the hybrid rings or Riblet couplers, and a succession of mitered corners. As a consequence of the considerable lengths of guide through which these reflections are transmitted, a rapid fluctuation of the standing-wave ratio with frequency is to be expected. This is confirmed

in Figure 66, where the match of the X-band model of the AN/SPS-2 seen in Figure 50 is plotted against frequency. The maximum standing-wave ratio is generally less than 3 db, which corresponds to a vswr of 1.4. The period of the variation has been correlated with the line lengths between the feed horns and the hybrid rings.

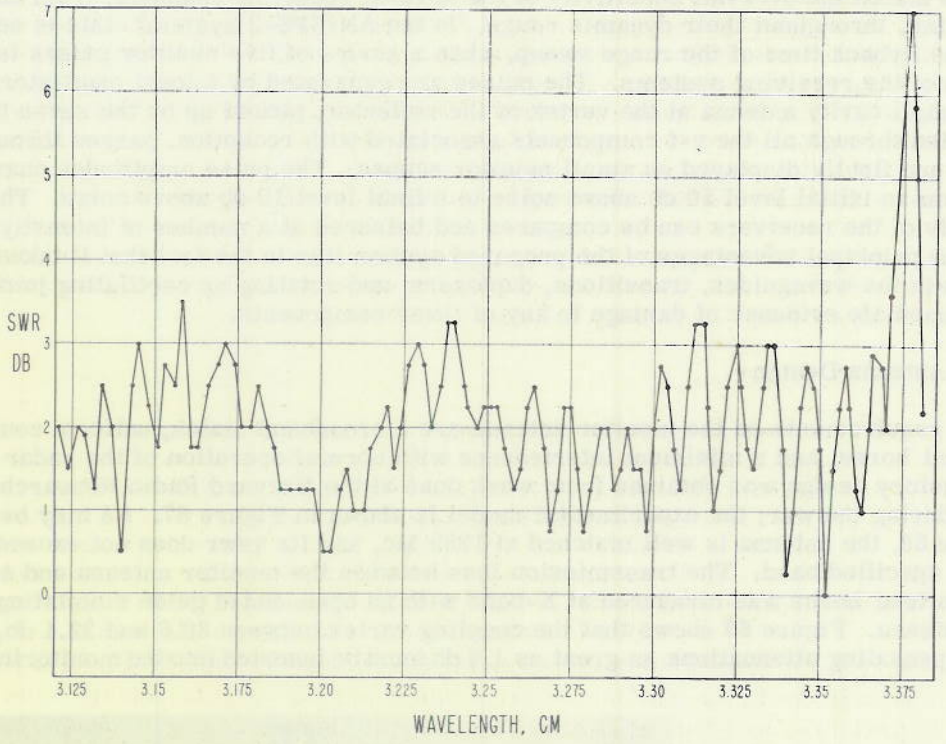


Figure 66 - Standing-wave ratio at input to power-division network

The feed system of the L-band model will be much shorter in terms of wavelengths, and the situation will be further improved by the use of Riblet couplers instead of hybrid rings. The feed horns can be matched to a certain extent by the use of a pressurizing cover, but on the other hand the effect of the polarization-twist duplexers is not included in this curve. It is hoped that an over-all vswr of less than 1.5 can be realized and that it will ensure satisfactory magnetron operation. However the large mismatch at a wavelength of 3.377 cm, where all the reflections appear to be additive, demonstrates the difficulty that can arise even with extreme care in matching the individual components. All unnecessary sources of reflection must be eliminated, even at the cost of considerable design effort.

Gain of the Transmitting Pattern

The gain at the maximum of the transmitting pattern was measured at midband and found to be 32.1 db, or 4.7 db down from the gain of the lower receiving beams. Since each of these beams received only a quarter of the transmitter power, a gain reduction of 6 db might have been anticipated. The improvement must result from contributions by neighboring beams.

## MONITOR ANTENNA

### Provisions for Monitoring Receiver Channels

To ensure accurate operation of a video-comparison height-finding system, it is necessary to match the over-all sensitivity of the several receiving channels, from antenna to video output, throughout their dynamic range. In the AN/SPS-2 system[9] this is accomplished during the flyback time of the range sweep, when a series of five monitor pulses is injected into each of the receiving systems. The pulses are generated by a local oscillator, radiated from a small cavity antenna at the vertex of the reflector, picked up by the seven feed horns, transmitted through all the r-f components associated with reception, passed through the receivers, and finally displayed on small monitor scopes. The pulse amplitudes change in 10-db steps from an initial level 50 db above noise to a final level 10 db above noise. Thus the sensitivity of the receivers can be compared and balanced at a number of intensity levels. One of the principal advantages of the proposed system lies in the fact that it takes account of losses in the waveguides, transitions, duplexers, and rotating or oscillating joints, and gives immediate evidence of damage to any of these components.

### Monitor Antenna Design

The requirements on the monitor antenna are a broadband match, uniform coupling to the feed horns, and a minimum interference with normal operation of the radar antenna. A satisfactory design was obtained from work done at the Harvard Radio Research Laboratory[10] during the war; the experimental model is shown in Figure 67. As may be seen in Figure 68, the antenna is well matched at 1285 Mc, and its vswr does not exceed 1.25 over the specified band. The transmission loss between the monitor antenna and each of the seven feed horns was measured at X-band with an open-ended guide simulating the cavity antenna. Figure 69 shows that the coupling varies between 30.6 and 32.4 db, so that compensating attenuations as great as 1.8 db must be inserted into the monitoring system.

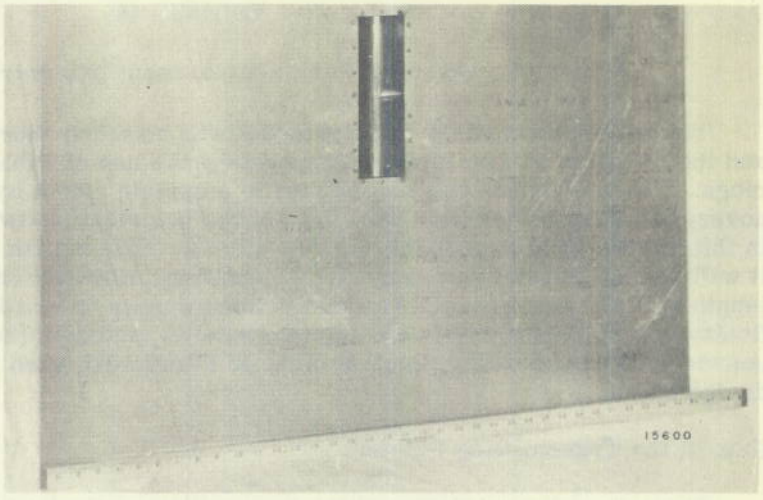


Figure 67 - Monitor antenna

[9] Ellis, R. E., "A Proposed Timing Control and Monitor System for the AN/SPS-2 Radar" (Confidential), NRL Report No. 3885

[10] Reich, H. J., ed., "Very High Frequency Techniques," New York, McGraw-Hill, 1947, pp. 185-189

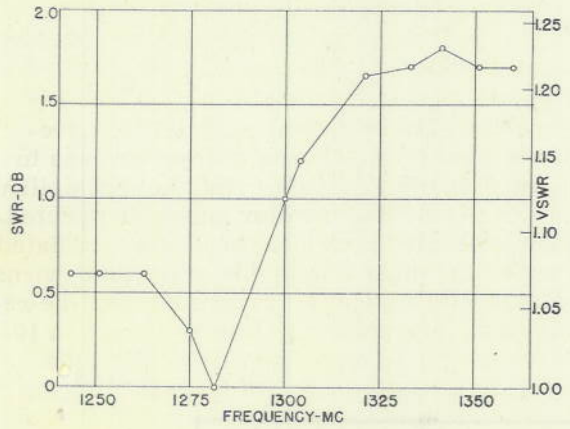


Figure 68 - Standing-wave ratio of monitor antenna

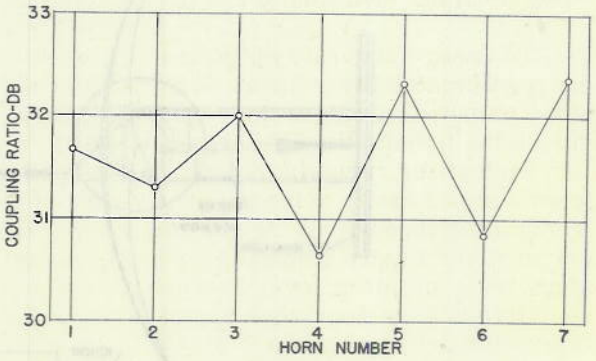


Figure 69 - Coupling ratio between monitor antenna and individual horns

The coupling between the cavity antenna in Figure 67 and an L-band model of a single feed horn, mounted at a distance equal to the focal length, was found to be 31.6 db at 1300 Mc. This result seems to indicate that the antenna reflector does not affect the general level of the monitor signal, although it may be responsible for the minor fluctuations seen in Figure 69.

## MECHANICAL DESIGN OF THE ANTENNA AT L-BAND

### NRL Drawings

At the conclusion of development work on the X-band model of the antenna, a set of outline drawings was prepared showing the significant dimensions of the reflector and feed system, scaled to the actual frequency of 1300 Mc. These drawings, together with all available performance data, were submitted[11] to the Bureau of Ships for forwarding to the General Electric Company, which has contracted for the production of two units of the AN/SPS-2 radar. Three of the drawings are reproduced in Figures 70, 71, and 72.

Figure 70 shows three views of the complete antenna, which is tilted upward $7^0$-6′ to bring the lower 3-db point of the first beam onto the horizon. The waveguide components are covered by a metal catwalk for convenience in servicing; hinged doors provide access to the duplexers and power-division network. The antenna for IFF Mark 5 mounted across the front of the platform is the 20-foot AN/AS-295 array. It must be modified to increase its vertical directivity and weatherproofed to meet Navy specifications.

Figure 71 shows the feed-horn assembly and the proposed method of mounting the pressurizing cup on a supporting structure which does not project beyond the horn aperture. The pressurizing cup might be secured by means of sheet-metal screws and sealed with a large rubber gasket.

---

[11] NRL Conf ltr C-3930-84/49 vlb, "Radar—SPS-2 Antenna—Electrical Design Specifications," November 28, 1949

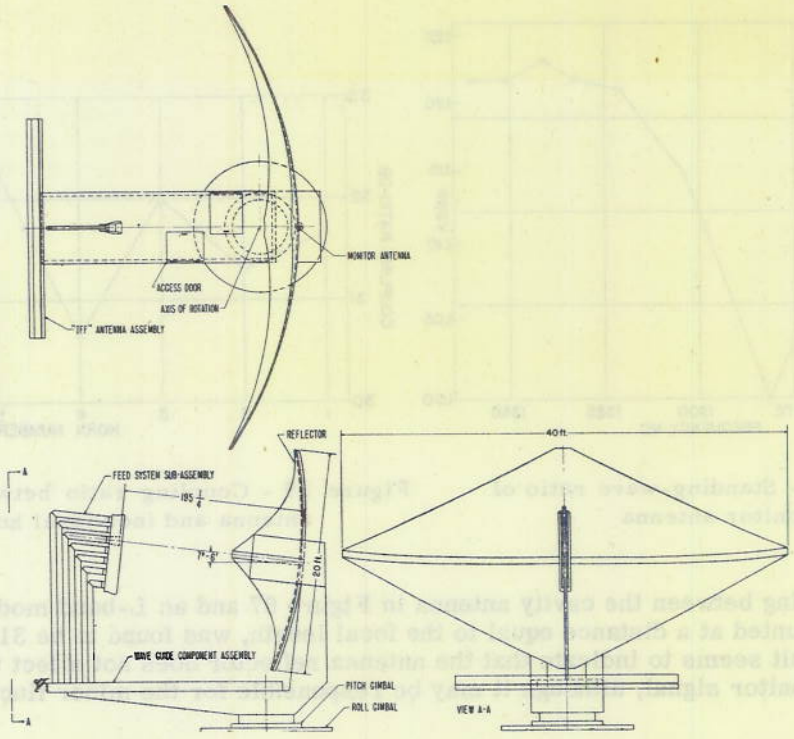


Figure 70 - NRL outline drawing of L-band antenna

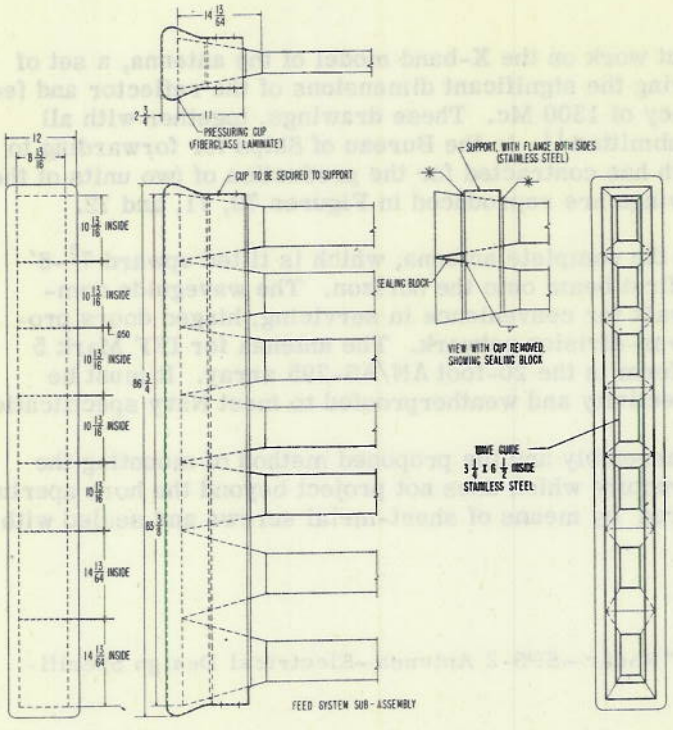


Figure 71 - NRL outline drawing of feed horns and pressurizing cover

Figure 72 is a layout of the waveguide components installed beneath the catwalk. The transmitter power is brought up through a $TM_{01}$ rotary joint at the right side of the drawing and passes into a hybrid-ring power-division network. Six of the seven channels contain folded sections of guide to accommodate phasing adjustments; the individual feed lines are of equal length as shown. The polarization-twist duplexers at the left of the drawing feed directly into the horns and are connected back to the receiving rotating joints through 1-5/8-inch coaxial lines.

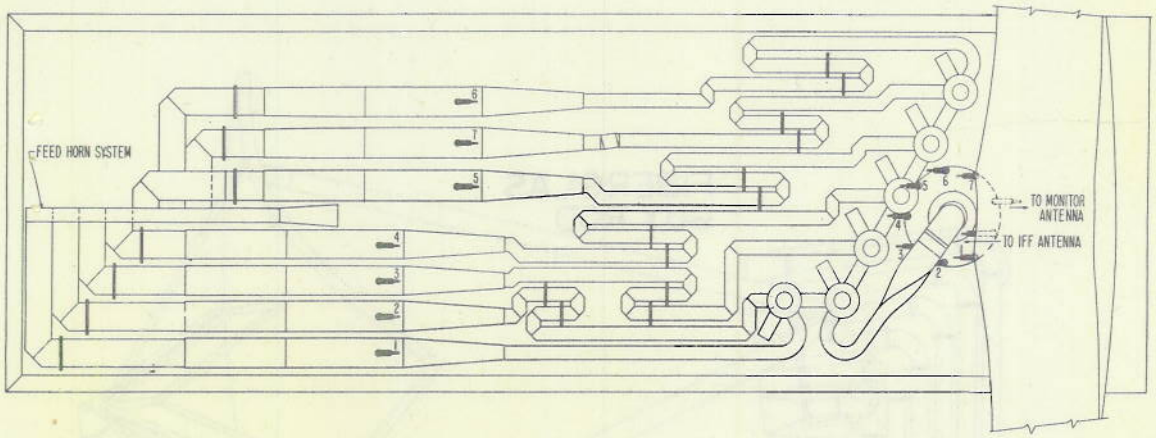


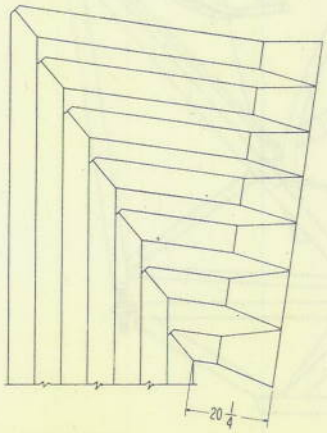


Figure 72 - NRL layout of waveguide components

AIL Drawings

Design of the production models of the AN/SPS-2 antenna has been subcontracted by General Electric to the Airborne Instruments Laboratory (AIL). One of their study drawings is reproduced in Figure 73. Mechanical considerations have dictated a number of small changes in the antenna configuration, some of which have been modeled at X-band to determine their effect on the r-f performance. These include:

1. Obstructions which increase the feed-horn silhouette

   a. Flanges used to assemble horns and bends

b. Beam used to keep bends in line

c. Mounting-bracket for guy rods

2. IFF antenna (not shown)

3. Glass-cloth laminate guy rods

4. Metal brace rods

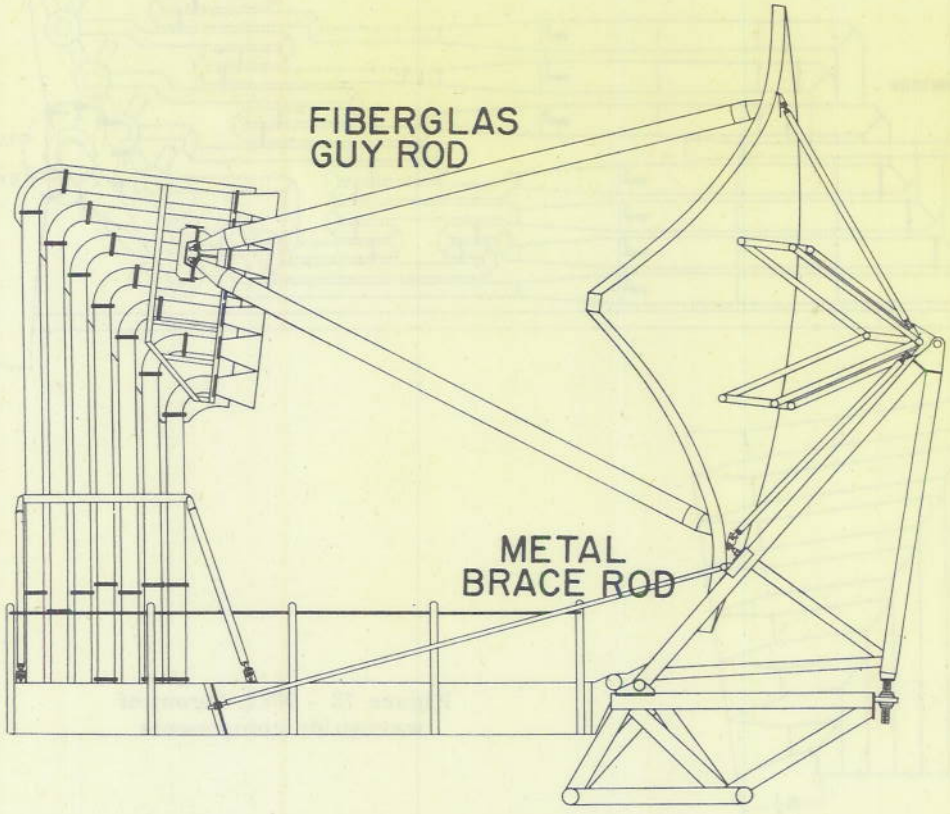


Figure 73 - Airborne Instruments Laboratory outline drawing of L-band antenna

Effect of Structural Members on Final Patterns

Since experience with waveguide flanges had indicated that obstructions alongside the feed horns would raise the sidelobe level in the horizontal patterns, the first item was regarded as particularly serious. Accordingly, the structures listed as 1a and 1b were scaled to X-band and installed on the feed assembly as shown at A, B, C, and E′ in Figure 74. Their effect on the horizontal patterns of beams 1 and 3 may be seen in Figures 75 through 78, while the highest sidelobes for each curve are listed in Table 7.

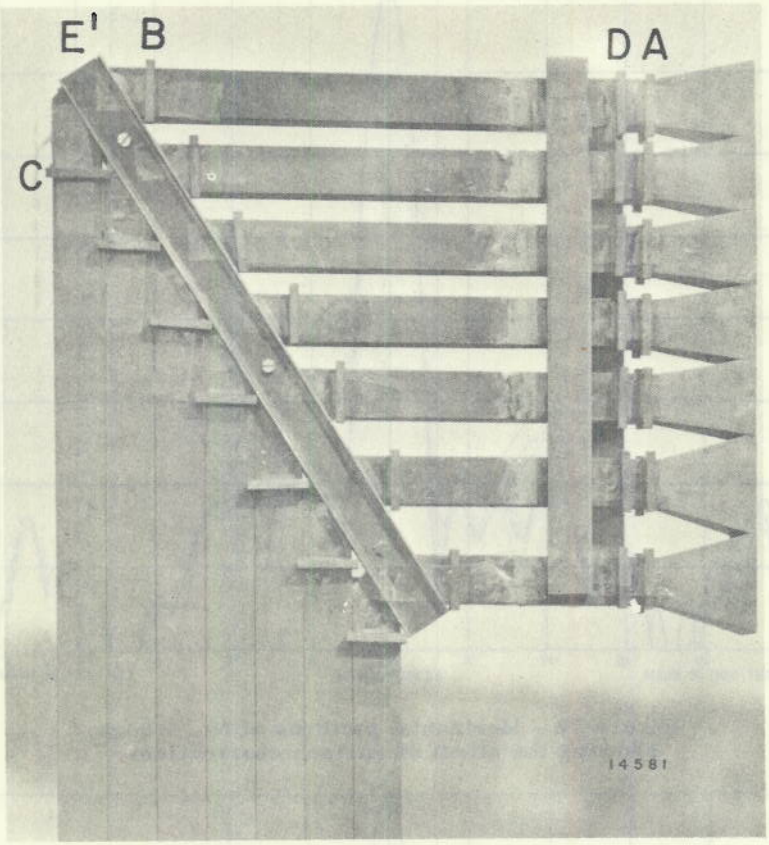


Figure 74 - X-band model of feed-horn assembly, showing obstructions tested

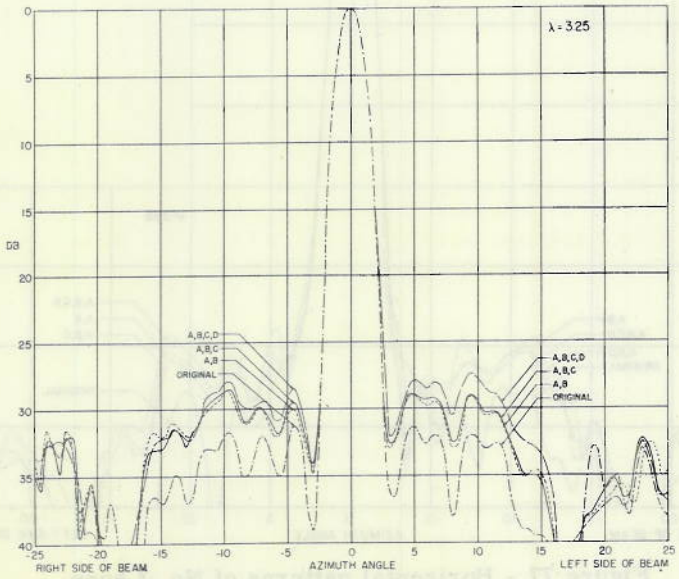


Figure 75 - Horizontal patterns of No. 1 horn, showing the effect of various obstructions

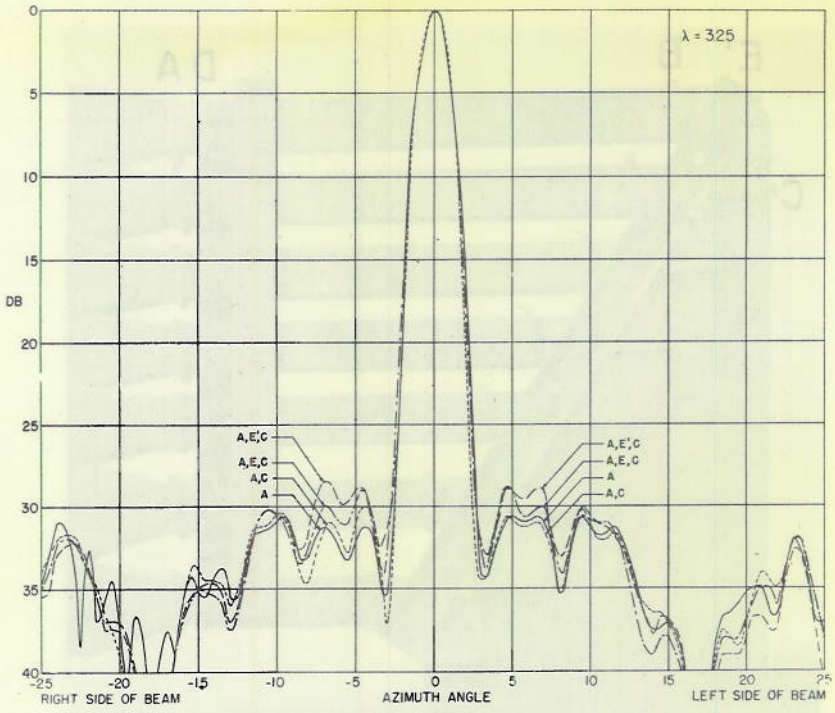


Figure 76 - Horizontal patterns of No. 1 horn, showing the effect of various obstructions

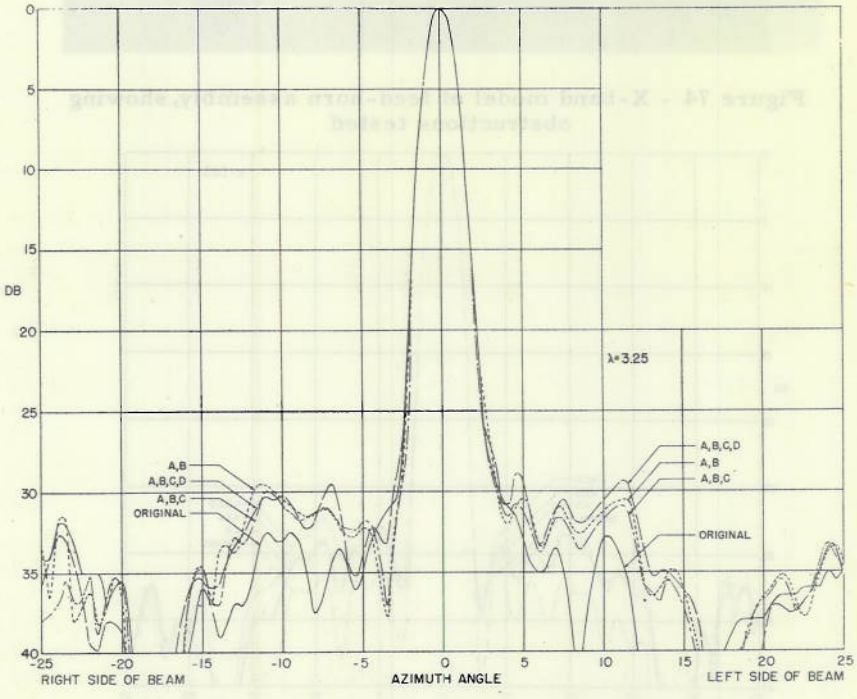


Figure 77 - Horizontal patterns of No. 3 horn, showing the effect of various obstructions

CONFIDENTIAL

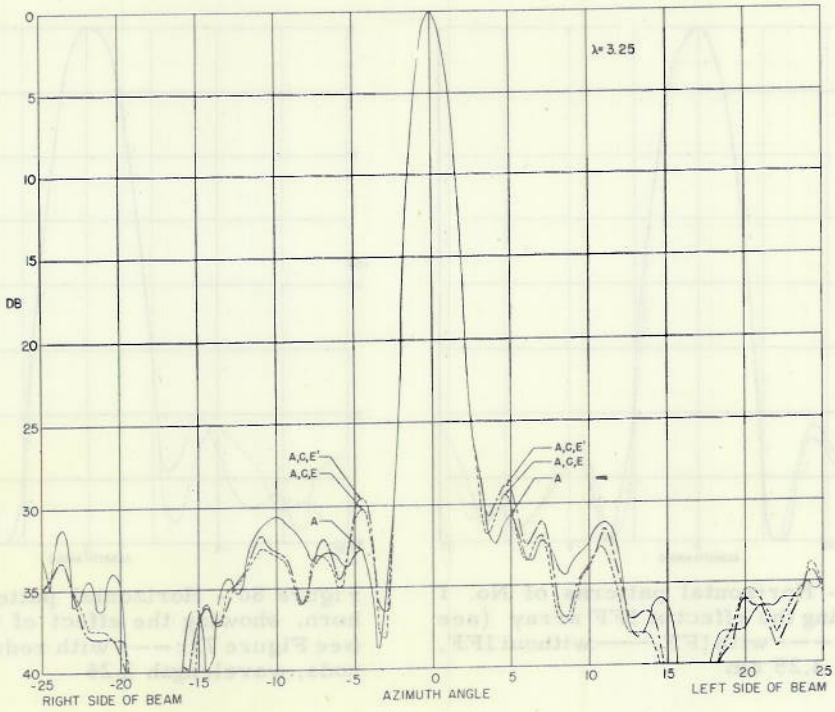


Figure 78 - Horizontal patterns of No. 3 horn, showing the effect of various obstructions

TABLE 7
Effect of Beam and Flanges on Horizontal Patterns

| Configuration | Highest Sidelobe (db) | |
|---|---|---|
| | Beam 1 | Beam 3 |
| Original | 31.3 | 32.5 |
| A | 30.6 | 30.7 |
| A + B | 28.6 | 29.5 |
| A + C | 30.0 | --- |
| A + B + C | 28.9 | 30.0 |
| A + C + E | 28.9 | 29.4 |
| A + C + E′ | 28.5 | 28.9 |
| A + B + C + D | 27.4 | 28.9 |

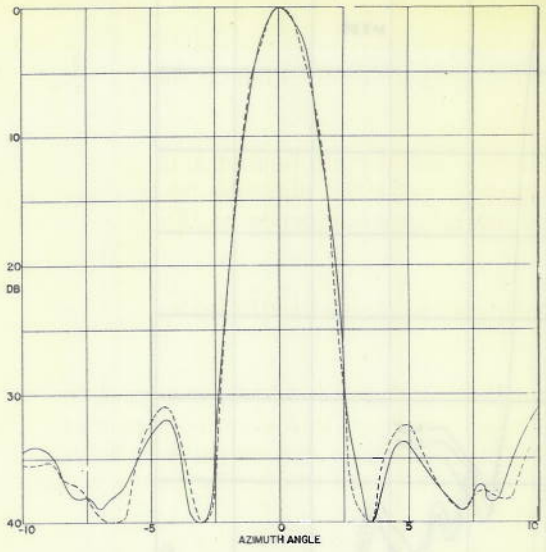


Figure 79 - Horizontal patterns of No. 1 horn, showing the effect of IFF array (see Figure 70): – – – with IFF, —— without IFF, wavelength 3.25 cm

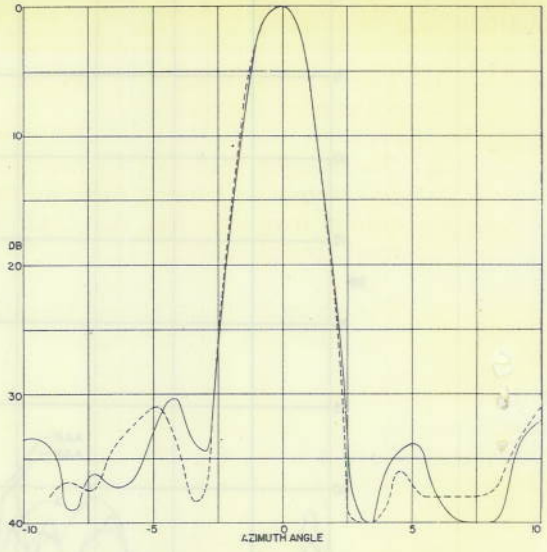


Figure 80 - Horizontal patterns of No. 1 horn, showing the effect of four guy rods (see Figure 73): – – – with rods, —— without rods, wavelength 3.25

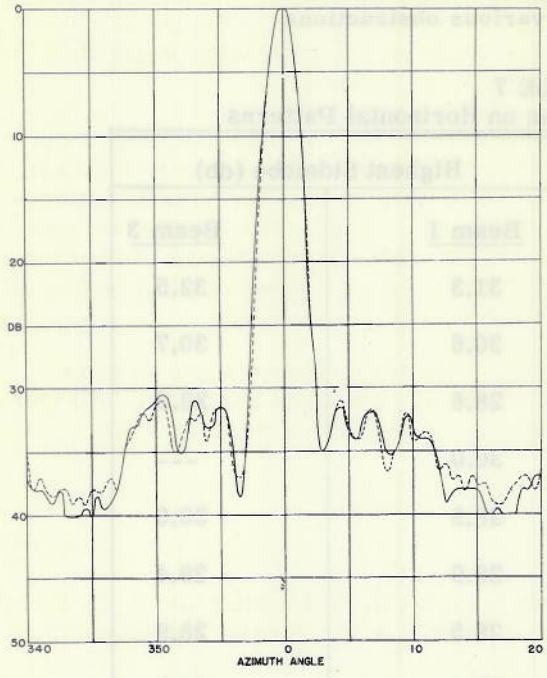


Figure 81 - Horizontal patterns of No. 1 horn, showing the effect of metal brace rods (see Figure 73): ——— with rods, – – – without rods, wavelength 3.25 cm

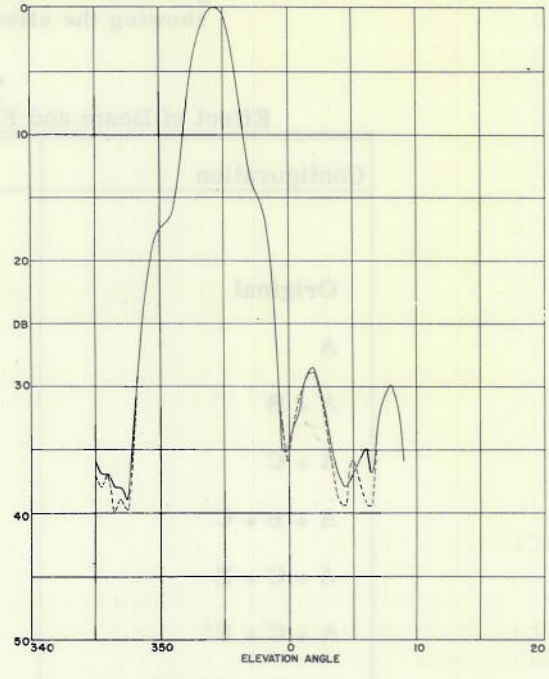


Figure 82 - Vertical patterns of No. 1 horn, showing the effect of metal brace rods: – – – with rods, ——— without rods, wavelength 3.25 cm

[redacted]AL

Symbol E refers to the channel beam turned with its smooth side out. The following conclusions may be drawn:

1. The vertical flanges (A, B, and D) have a greater effect than do the horizontal flanges (C).

2. The dummy flanges (D), mounted a quarter-wavelength behind A in an attempt to compensate for its scattering, raise the sidelobe level rather than lowering it. Evidently the interference depends on the total frontal area.

3. The channel beam should be mounted smooth side out to eliminate one source of scattering.

If it were possible to limit the installation to beam E and flanges A and C, the sidelobe level would be approximately 29 db on beams 1 and 3. However, this compromise was not acceptable to AIL representatives, who felt that flange B was also essential. With this addition, the sidelobes would reach 28 db on both beams, and the performance would be marginal.

An alternative solution, suggested by the fact that the sidelobe level depends on the frontal area of the obstructions, is to cover the beam and flanges with a thin sheet-metal fairing, terminated at the front edge against the flare of the horns. One of these cover plates is shown on the far side of the feed assembly in Figure 73; the one on the near side has been removed to show the structural details. The fairing was modeled at X-band by beveling two sheets of 1/8-inch brass and soldering them to the feed structure as shown in Figure 3. A mounting bracket for the glass-cloth laminate guy rods is also in evidence in this photograph. Horizontal patterns obtained with this arrangement are shown in Figure 26, where the highest sidelobe is seen to be 30.5 db down. In view of the excellent results obtained, it is anticipated that AIL will use cover plates in the production models.

Model tests show that if an AN/AS-295 IFF array is mounted across the front of the antenna with its lower edge resting on the catwalk, the horizontal sidelobes may increase as much as 1 db, and that the guy rods of Figure 73 have a negligible—or even beneficial—effect on these lobes. The results are shown in Figures 79 and 80. These patterns were taken at an early stage of the development, and should be interpreted in terms of the changes in sidelobe level rather than accepted as representative values. No serious difficulty is anticipated from either of these structures.

Figures 81 and 82 are horizontal and vertical patterns of the lowest beam with the feed configuration shown in Figure 3, taken with and without the metal brace rods of Figure 73. There is no significant effect; the patterns are quite satisfactory in either case.

## ACKNOWLEDGMENTS

Important contributions to this work have been made by K. S. Kelleher and H. D. Fleming. The authors acknowledge numerous helpful discussions with A. A. Varela, who established the antenna requirements.

* * *





NAVY-DPPO PRNC. WASH., D.C.

[redacted]